TAMPEREEN TEKNILLINEN YLIOPISTO
TAMPERE UNIVERSITY OF TECHNOLOGY

PRADEEP GANESH
Impact of Nonlinear Distortion in Pulse-Doppler Radar Receivers
Master of Science Thesis

Examiners:
Professor, Dr.tech. Mikko Valkama
M.Sc. Markus Allen

Examiners and topic approved by the Faculty Council of the Faculty of Computing and Electrical Engineering on 6th February 2013

ABSTRACT

Tampere University of Technology
Master's Degree Programme in Electrical Engineering
PRADEEP GANESH: Impact of Nonlinear Distortion in Pulse-Doppler Radar Receivers
Master of Science Thesis, 51 pages, 1 Appendix page
June 2013
Major: Radio Frequency Electronics
Examiner(s): Professor, Dr.tech. Mikko Valkama
M.Sc. Markus Allen
Keywords: Direct conversion receiver, Pulse doppler radar, Non-linear distortion

The aim of the thesis is to study the applicability of Direct Conversion Receiver (DCR) in radar, as these receivers possess the advantage of reduced complexity and fewer bandwidth limiting components compared to the superheterodyne receiver. As the wireless technology, it is also necessary to study about the receiver functionalities in radar using Digital Signal Processing (DSP) techniques. In today's radar technology, designing the front end part of the radar receiver is more challenging, especially radar employing DCR, as these receivers are more prone to non-idealities such as I/Q Imbalance, non-linear distortion, DC offset and phase noise thereby affecting the dynamic range of the received echo signal. The pulse doppler radar is chosen in the thesis, as these radars are coherent, also capable of multiple target detection and provide large unambiguous range.

The objective of the thesis is to analyse the effect of non-linear distortion such as second and third order distortion and observing the effects of these non-linearities in post-processing blocks. In this thesis baseband non-linearities in I and Q branches of the radar receiver are more specifically addressed than the RF non-linearity and blockers. The analysis is carried out in such a way that, the basic mathematical expressions for the RF signal in the transmitter part and received echo signal at baseband considering the effect of doppler are modelled. The second and third order non-linearities are modelled with some special cases by introducing some imbalances in I and Q branches and the effect of increasing the doppler frequency beyond the specified Pulse Repetition Frequency (PRF) is to be analysed.

The effects of non-linearities are observed in post-processing blocks of the pulse doppler radar receivers. Thus, the final stage in the radar receiver blocks includes matched filtering or pulse compression and doppler processing as they are capable of separating target and clutter. The matched filtering or pulse compression follows Linear Frequency Modulation technique (LFM) as it is simple to generate the signal and insensitivity to doppler shifts. The pulse compression or matched filtering maximizes the Signal-to-Noise Ratio (SNR) by reducing the sidelobe levels using appropriate weighting functions so as to improve the resolution of the target. The doppler processing is capable of separating the target and clutter thereby improving the Signal-to-Clutter Ratio (SCR). The target signal is recorded and observed in a Range/ Doppler (R/D) matrix where the various parameters such as range, doppler information that includes measuring the doppler shift and radial velocity, location of the target etc. can be estimated. Other than the parameter estimation, the effect of non-linearities is observed in the R/D matrix. Comparisons of ideal scenario and non-ideal scenario and tabulations illustrating the comparison of second and third order distortion profiles are illustrated in the thesis to study about the performance and practicality of the radar receivers.

PREFACE

I would like to express sincere thanks to my Professor Dr.Tech. Mikko Valkama who has given me the opportunity to work in the department of Communication Engineering and for providing me constant supervision, guidance and always have been a source of inspiration for working on the thesis topic. I am extremely grateful to Markus Allen who has been constantly providing guidance, insight and motivation throughout my thesis work. I appreciate the support provided by George Vallant, Cassadian for providing guidance to work in the field of radar technology. I would also like to thank all my friends Saiful Islam, Basanta Pandey, Artur Brutyan, Duc Nguyen Thanh and Lutfi Samara for providing me recreational support and fruitful discussions till the end of my thesis. My sincere gratitude to my parents and my sister who has been constantly supporting and encouraging me in all endeavours.

Pradeep Ganesh
May 2013

TABLE OF CONTENTS

LIST OF FIGURES

LIST OF TABLES

LIST OF ABBREVIATIONS AND ACRONYM

A/D	Analog to Digital
AGC	Automatic Gain Control
AWGN	Additive White Gaussian Noise
BPF	Bandpass Filter
CA-CFAR	Cell Averaging Constant False Alarm Rate
CAGC	Clutter Automatic Gain Control
CFAR	Constant False Alarm Rate
CNR	Clutter-to-Noise Ratio
COHO	Coherent Oscillator
CSF	Channel Select Filter
CW	Continous Wave
D/A	Digital to Analog
DC	Direct Current
DCR	Direct Conversion Receiver
DCT	Direct Conversion Transmitter
DFT	Discrete Fourier Transform
DSP	Digital Signal Processing
DSPs	Digital Signal Processors
DTFT	Discrete Time Fourier Transform
FFT	Fast Fourier Transform
FMCW	Frequency Modulated Continous Wave
FPGA	Field Programmable Gate Array
I/O	Input/Output
I/Q	Inphase/Quadrature
IC	Integrated Circuit
IF	Intermediate Frequency
INS	Inertial Navigation System
IR	Image Reject
LFM	Linear Frequency Modulation
LNA	Low Noise Amplifier
LO	Local Oscillator
LPF	Lowpass Filter
MGC	Manual Gain Control
MTI	Moving Target Indicator
NAGC	Noise Automatic Gain Control
NLFM	Non Linear Frequency Modulation
PDI	Post Detection Interference
PRF	Pulse Repetition Frequency
PRI	Pulse Repetition Interval
PSF	Preselection Filter
PRT	Pulse Repetition Time
PSR	Peak Sidelobe Ratio

R/D	Range/Doppler
RADAR	Radio Detection and Ranging
RCS	Radio Cross Section
RF	Radio Frequency
RFI	Radio Frequency Interference
RSP	Radar Signal Processor
SCR	Signal-to- Clutter Ratio
SNR	Signal-to-Noise Ratio
STALO	Stable Local Oscillator
STC	Sensitivity Time Control

LIST OF SYMBOLS

$\phi(t)$	Time varying phase
φ_0	Progressing phase shift
$f(t)$	Instantaneous phase
f_d	Doppler Frequency
$x(t)$	Baseband signal before upconversion
$x_{RF}(t)$	RF signal after upconversion
$y_{RF}(t)$	RF Received signal
$y(t)$	Baseband downconverted signal
δR	Rayleigh resolution
dB	Decibels
Hz	Hertz
Δ_{AZ}	Azimuth angle
Δ_{EL}	Elevation angle
$f(t)$	Instantaneous phase
τ_t	Transmit pulse width
τ_g	Gate width
τ_s	Gate spacing
P_{f_1}	Input power levels at fundamental frequency f_1
P_{f_2}	Input power levels at fundamental frequency f_2
P_{IP}	Power level of third order intercept point
f_s	Sampling Frequency
$y_{weighted}^{LFM}$	Linearly weighted matched filter response
$w(f)$	Weighting function
Δ_{AZ}	Azimuth angle
$S(f)$	Received echo signal
$R(f)$	Reference signal
V_T	Threshold value
P_{fa}	Probability of false alarm rate
σ^2	Noise power
$A(t)$	Amplitude of the LFM waveform
B	Bandwidth of an LFM Signal
P_{IP}	Power level of third order intercept point
τ	Pulse width
f_0	Centre frequency
$V_{relative}$	Relative radial velocity
I	Inphase component of complex signal
Q	Quadrature component of complex signal
a_2	Second order constant in I-branch

b_2	Second order constant in Q-branch
a_3	Third order constant in I-branch
b_3	Third order constant in Q-branch
R_{max}	Maximum unambiguous range
T_P	Pulse Repetition Rate
f_0+f_d	Positive doppler shift
f_0-f_d	Negative doppler shift
T_d	Total duration of finite pulse trains
c	Velocity of electromagnetic wave
λ	Carrier wavelength
ε_r	Relative permittivity
τB	Time-bandwidth product
B/τ	LFM Coefficient
ω_{LO}	Local Oscillator frequency

1. INTRODUCTION

The word 'RADAR' is an acronym that stands for Radio Detection and Ranging. In early days, the radar functionality was confined to detecting the target and determining the range. As the advancement of science and technology, there has been a tremendous evolution in the radar technology. The radar used at present days is more efficient as they are equipped with sophisticated transducers and computer systems.The modern radars suppress the clutter and jammers present in the signal. The applications of radars in olden days include military and tracking civilian aircrafts and vehicles whereas the modern radars are capable of mapping either two or three dimensionally, monitoring the earth resources, collision avoidance etc [1].

The radar technology has led to the development of microwave technology as the radar requires transmitter and receivers with proper antennas. The radar performance has been improving since decades as the radar employs advanced technology such as microwave technology, DSP and ICs. Modern communication systems and signal processing has been playing a vital role for detecting the targets with a background of active clutters. Thus, traditional techniques have been playing a key role in order to achieve modern techniques in radar. The non-linearities that arise in radar cause large interference by affecting the small desired signal and it is difficult to resolve the target from the interference. Some active interference cancellation methods can be implemented in the radar so that the location of the targets can be identified with good resolution. For avoiding the jamming effect, frequency agility is implemented in radar [2]. At recent times, the radars are employed with highly sophisticated processors with efficient algorithms that provide better radar performance. Single channel radar requires many processors as the I/O requirements are high. Multicore processors are at high demand at present [3].

1.1. Thesis Objectives and Significance

The main aim of the thesis is to study the applicability of DCR in radar and to study the effect of non-linearities on radar receivers that is tested using computer simulations.The effect of non-linear distortion on the radar receiver is the main goal of the thesis as the non-linear distortion is capable of masking the targets and produces false targets.

Implementing DCR is a challenge in radar. At present, most of the researchers are keen in implementing DCR in radar as they are not bulky, reducing the radar size. But there are challenges in implementing as the DCR are more prone to RF impairments such as I/Q imbalance, non-linear distortion, DC offset and phase noise. The thesis addresses specifically on intermodulation distortion, due to the non-linearities affecting

the desired band of analysis generating second and third order products. The thesis mainly focusses on baseband non-linearities that are produced in I and Q branches of DCR. The thesis investigates the ideal case and non-ideal case in radar by observing the spectrum in R/D matrix. Thus, the thesis helps in understanding the effect of non-linear distortion in radar and also helps in understanding the overall functionality of radar receiver.

1.2. Thesis Structure and Method

The thesis is organized in such a way that, chapter 2 deals with radar receivers that employs DCR with post-processing blocks such as pulse-compression or matched filtering and doppler processing. The most common waveform modulation is the LFM, as the modulation technique is capable of tracking the target with high resolution. The common receiver architectures such as heterodyne and homodyne receivers are explained with proper functionality in radar. As the thesis deals with second and third order distortion, the concept about the signal strength is explained in the receiver dynamic range.

The chapter 3 deals with pulse doppler radar as the thesis revolves around DCR in pulse doppler radar. The section under chapter 3 explains about the overall functionality of pulse doppler radar with transmitter, receivers and post-processing blocks.The location of target, interferences, non-linearities, jammers etc. can be analyzed in doppler spectrum for the corresponding range. The concepts of range gates are presented. Selection of PRF and its ambiguities due to low, medium and high PRF and resolving the ambiguities are discussed.

The chapter 4 describes about the basic modelling of RF and baseband signal in the radar transmitter and receiver. The chapter also focuses on modelling of each RF imperfections in homodyne receivers in a pulse doppler radar. Some of the common RF imperfections in pulse doppler radar are I/Q- Imbalance, non-linear distortion, DC offset and phase noise. The effect of each RF imperfections in pulse doppler spectrum is discussed in each section. The effect of I/Q imbalance in a zero IF- radar receivers is already presented by Schneider [8]. As the thesis concentrates on non-linear distortion affecting the desired signal, modelling of second and third order distortion in I and Q branches are illustrated.

The chapter 5 focusses on the simulation results that are obtained by simulating the ideal and non-ideal case of a radar receiver. Each functional block of a radar receiver is simulated in ideal scenario and the results are illustrated. In non-ideal case, the second and third order non-linearities are modelled in baseband and its corresponding effects are studied in R/D matrix. Effect of non-linear distortion in I and Q branches including the effect of imbalances in I and Q branches are illustrated. The effect of increasing the doppler frequency than the specified PRF, that results in doppler ambiguity is also illustrated.

2. RADAR WAVEFORM AND RECEIVERS

Radar is an object detection system for locating the targets that are far away from the observer. The electromagnetic sensor comprises of transmitter and receiver for detecting the reflected objects. The function of detection and location of objects is performed by radiating a series of pulses or electromagnetic energy from an antenna. The signal from the antenna is transmitted into space. The series of pulses that are radiated, hits the object that is to be detected, called the target. The signal is reflected from the target in many directions. The received radar signal comprises of desired echo signal and the undesired interferference. The undesired interference is removed from the desired echo signal by the radar receiver where the received signal is amplified, filtered, downconverted and finally the echoes are digitized. The sources that constitute interference are noise that are generated within the radar receivers and also include the noise from galactic sources, communication equipments and radars that are adjacent to each other. Undesired interference is also part of radar signal that is scattered due to the presence of undesired targets or object, which leads to scattering of radar signal or attenuation of the radar signal, called the clutter [1].

In this chapter, the general configuration of radar that operates on homodyne receiver is discussed, as the thesis concentrates on DCR as shown in Figure 2.1. In general, the radar receiver is implemented using superheterodyne receivers, whereas the implementation using direct conversion receivers are tried with best efforts so that the complexity is reduced and less bandwidth components are required [9]. The information about the target is present in the radar signal. Thus, it is important to know about the characteristics of the signal and the waveform types that are employed in radar system. A layout of homodyne and heterodyne receivers are explained to know the difference in operation of the receivers. As the thesis revolves around homodyne receivers, the necessity of homodyne receiver in radar is a must to be known. Dynamic Range, a key parameter in radar receiver, represents the signal strength of radar, so that the performance of the radar receiver can be estimated.

2.1. General Radar Structure

The general structure of radar comprises of transmitter, antennas, duplexer, receiver and post-processing blocks. The DCT act as a radar transmitter by providing necessary power amplification for the signal to be transmitted as shown in Figure 2.1. The DCT converts the baseband signal to RF with zero IF component .The transmitted signal is measured by average power in milliwatts or megawatts. Thus, the average power is a

parameter that estimates the performance of radar. The average power is a better measurement tool than peak power.

In radar, single antenna is shared between transmitter and receiver, so that short pulse wave is transmitted and received. In radar, duplexer performs the function of allowing transmitter or receiver to function at a time. The sensitive receiver is protected, if the transmitter is switched on and the transmitter is protected from the reflected signal from the target, if the receiver is switched on. Thus the duplexer acts as a switch between transmitter and receiver [10].

The propagation of electromagnetic signals into space by the transmitter and the reception of echo signals by the receiver are accomplished by the antenna. Directive antenna is implemented in the radar receiver, so that narrowbeam is concentrated, to estimate the direction of the target. Generally, a transmitter emits a narrow directive beam whereas a receiver receives echo signals that have large area. Spatial filtering is a characteristic of antenna in radar where it provides angle resolution and other capababilities.

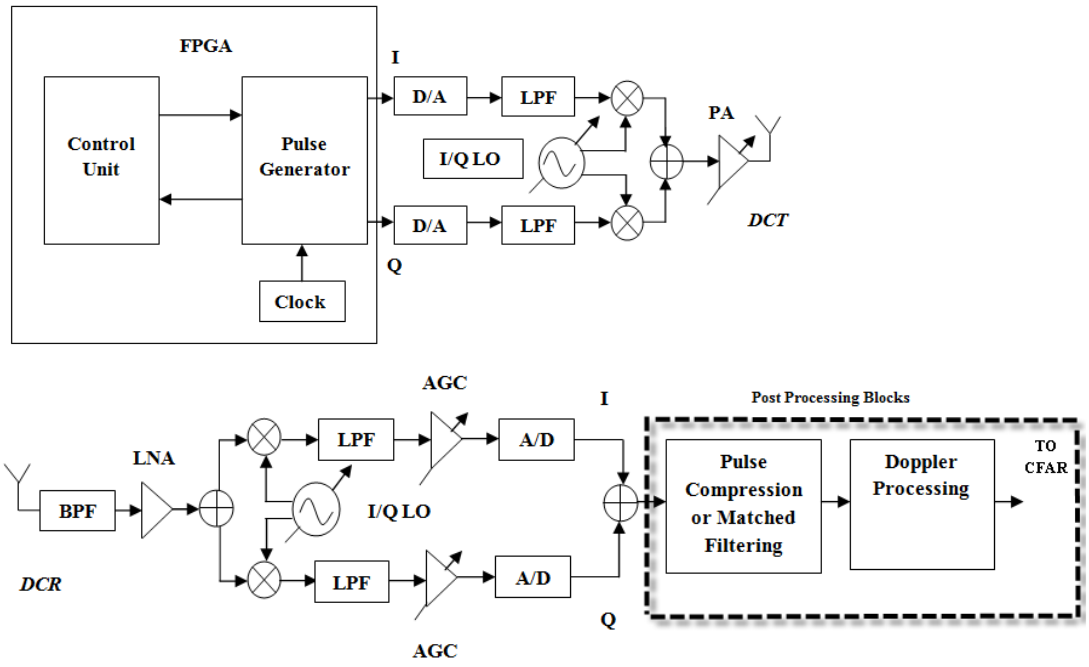

Figure 2.1. *Block diagram of simple radar transceivers*

The DCR converts RF to baseband signal. The amplification of weak signal to a desired level is carried out by the receiver. The detection decision and information extraction about the target from the noise is important aspect in radar, as noise is the limitation in radar. Other than the noise, echo signals due to false targets termed as clutter, is also a major limitation in radar. Thus, dynamic range of the radar has to be high enough so that saturation of the radar receiver can be prevented. Dynamic range is a measure of signal power level, that indicates the ratio of maximum signal level to the minimum signal level and the unit of dynamic range is dB.The value of maximum signal level can be estimated by, measuring the tolerance level of non-linear effects of receiver response.

Signal processor performs the task of removal of undesired signal that degrades the detection process. Matched filtering, doppler processing and detection decision are the stages that are included in processing of signals. Matched filtering involves maximizing the SNR. If the presence of clutter is larger than the receiver noise, separation of the moving target from clutter echoes is carried out by doppler processing. Thus, doppler processing involves improving the SCR of a moving target. The detection decision is the final step of signal processing in radar. In detection decision, a threshold value is set. The target is said to be present, if the receiver output exceeds the value of threshold. The chance of excessive false alarm is due to low value of threshold. Some targets would be missed, if the threshold value is high. The threshold value is set so that there is proper predetermined average rate of false alarms due to the receiver noise [13].

In the post processing stage, the signal is processed to track the path of the target. To display the track locus of target locations, data processing is implemented. The processed signal is further examined in a display for examining the nature of the target. The timing signals are provided by the radar control, so that the radar works in a coordinated manner.

The post processing block includes pulse compression or matched filtering, doppler processing and CFAR detection as shown Figure 2.1. The main motive behind the concept of pulse compression technique is to compress the long duration pulse to short duration pulse for better range resolution and easy detection of targets [14]. Continous phase modulation is the type of modulation employed mostly in all pulsed radar systems. The continous phase modulation is such an efficient technique that provides large peak power and good range resolution. Matched filtering is performed to maximize the SNR in the radar signal. The continous phase modulation can be classified into two types as LFM and NLFM. The LFM signal or chirp signal is the most widely used continous phase modulation, as it is easy to generate signal and very less sensitive to doppler shifts. Other than the mainlobe, the matched filter output has the presence of sidelobes. These sidelobes are often mistaken as targets. The sidelobe suppression is generally carried by linear and non-linear sidelobe reducing technique called the apodization [15]. The general way to suppress sidelobe is using the linear amplitude weighting functions. The general weighting functions used are rectangular, hamming and hann windows [16]. The pulse compression ratio or time-bandwidth product is a measure of the pulse compression in a signal and given as $\beta\tau$, where β is the bandwidth of the transmitted pulse and τ is the pulse width. The output of the LFM matched filter is a *sinc* function for the high values of compression ratios whereas for the low value of compression ratios, *sinc* function is not obtained as the sidelobes are not suppressed. In NLFM techniques, matched filtering apodization techniques are not required for sidelobe suppression as the modulation provides reduced sidelobes [15]. Linearly weighed matched filter response is given by [15],

$$y_{weighted}^{LFM} = FFT^{-1}\left\{S(f)\times(w(f)\times R^{*}(f))\right\} \tag{2.1}$$

where *W(f)* is the weights, *S(f)* is the received echo signal, *R(f)* is the reference signal for matched filtering [15].

The CW radars and pulse doppler radars employs doppler processing. In a simple way, the purpose of doppler processing can be understood by considering CW radars that utilizes a pure sine waveform of the form $\cos(2\pi f_0 t)$. On analyzing the received signal for the stationary target in frequency domain, the presence of target and clutter is present at the centre frequency f_0. For moving, targets, the centre frequency for the target is shifted by f_d, doppler frequency. Thus, on measuring the difference between the f_0 and f_d, obtains the value of doppler shift and estimating the target radial velocity [11]. Thus, it easy is to detect target in high clutter environment by increasing the value of SCR.

Doppler processing can be explained using pulse doppler radars. The concept behind the doppler processing is that, a mapping is created called the R/D matrix or R/D map. The footprint is obtained by intersecting the antenna 3dB beamwidth with the ground. The R/D matrix is divided into resolution cells. The range and doppler frequency are the sides of the matrix. Range gating and pulse compression provides the range resolution ΔR. Coherent signal processing provides the frequency resolution Δf. The matrix is created in such a way that N_a is the number of doppler cells or azimuth cells and N_r is the range bins. Thus, a map of matrix size $N_a \times N_r$ is generated, where N_a is present in rows and N_r in columns. On exposing the targets to antenna beam, the echoes received from the target are stored in corresponding range bins. From the corresponding range bins, the echoes are mapped into the first row of the map. Before the next pulse is transmitted, the data present in the first row is incremented to the second row. The process continues, till the last pulse is received. Thus, last row of the matrix has the data of received signal of first transmitting pulse and the first row of the data has the presence of received signal of last transmitting pulse. For an object in motion, the targets can be resolved by taking FFT of the corresponding range bins at dwell time. A peak is obtained for the particular target at that range and doppler frequency within a resolution cell.

There is a presence of some amount of clutter after the pulse compression and doppler processing. The clutter may be due to the rain, snow and may be due to the devices involved in signal processing. Due to the presence of clutter, the target is masked with presence of interference that leads to false alarms. The remaining amount of clutter can be removed by CFAR methods [13]. In CFAR, a threshold value is set. The threshold value is set so that the probability of false alarm is maintained constant. The threshold value, V_T and probability of false alarm, P_{fa} is given by the relation [11],

$$V_T = \sqrt{2\sigma^2 \ln\left(\frac{1}{P_{fa}}\right)} \tag{2.2}$$

The above equation (2.2) holds true for the case, noise power σ^2 is constant. But this condition is not exactly true. The noise variance is not constant and the threshold value

must be updated so that probability of false alarm is maintained constant. This is called CFAR [11]. If the signal level is higher or equal to the threshold, target hit vector is 1. If the signal level is lesser than the threshold level, target hit vector is 0.

2.2. Linear Frequency Modulation (LFM) Signal

The uniqueness of the LFM is that it makes the radar to search and track the targets with high resolution. The LFM has an important property called the Doppler tolerance. The waveform experiences stretch processing that process extremely high bandwidth waveforms for high resolution [1]. The modern radar systems employ LFM in order to achieve higher operating bandwidths. The traditional radar systems employ frequency or phase modulated signals. In LFM, frequency is varied with reference to time. If the frequency is swept upward with reference to time it is called an up-chirp whereas if the frequency is swept downwards with reference to time, it is called a down-chirp as shown Figure 2.2 [11].

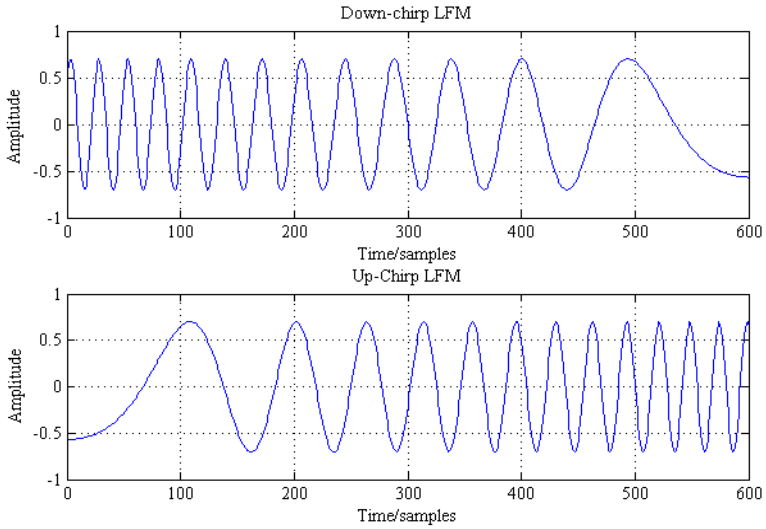

Figure 2.2. *Down-chirp and Up-chirp LFM waveforms*

The time domain analysis of LFM is illustrated in the following pages. The time domain analysis of LFM signal is analyzed in baseband. Considering a LFM pulse at baseband frequency with amplitude *A*, bandwidth *B* and pulsewidth τ of the waveform,

$$x_I(t) = A\cos(\pi \frac{B}{\tau} t^2) \text{ and } x_Q(t) = A\sin(\pi \frac{B}{\tau} t^2) \qquad \frac{-\tau}{2} \le t \le \frac{\tau}{2} \tag{2.3}$$

In the radar transmitter, the radar transmits baseband to RF signal is given as [1],

$$x_{RF}(t) = A\cos(2\pi f_0 t + \pi \frac{B}{\tau} t^2) \qquad \frac{-\tau}{2} \le t \le \frac{\tau}{2} \tag{2.4}$$

In the radar receiver, complex downconversion takes place before the pulse compression stage such that the RF signal is converted to a baseband signal where I and Q components are obtained. The signal at baseband is given as [1],

$$x(t) = A\exp(j\pi \frac{B}{\tau} t^2) \qquad \frac{-\tau}{2} \le t \le \frac{\tau}{2} \tag{2.5}$$

In LFM, phase of the signal is varied with respect to time. Thus on considering phase of the above equation (2.5),

$$\phi(t) = \pi \frac{B}{\tau} t^2 \qquad \frac{-\tau}{2} \le t \le \frac{\tau}{2} \tag{2.6}$$

On differentiating the above equation (2.6) with respect to time, instantaneous frequency is obtained, that is given as,

$$\frac{d\phi(t)}{dt} = 2\pi \frac{B}{\tau} t \qquad \frac{-\tau}{2} \le t \le \frac{\tau}{2} \tag{2.7}$$

Thus, the instantaneous frequency is given as [1],

$$f(t) = \frac{B}{\tau} t \qquad \frac{-\tau}{2} \le t \le \frac{\tau}{2} \tag{2.8}$$

In simple words, it can be said that instantaneous frequency varies linearly with respect to time. This is called LFM. The LFM signal is also called the chirp signal as the signal generates a chirping sound at the audible frequency range.

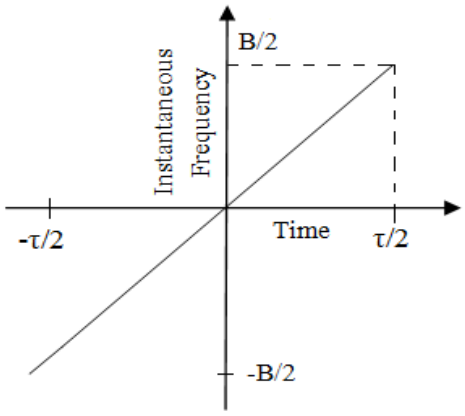

Figure 2.3. *Time vs Instantaneous frequency plot of an LFM signal [1]*

The above Figure 2.3 and the above equation (2.8) represent the plot of instantaneous frequency with respect to time. It can be observed that an LFM signal of bandwidth B is swept at pulse width of τ seconds. From the equation (2.8), B/τ is called the ramp rate or sweep rate that is obtained from the slope of instantaneous frequency.

$$X(\omega) \approx |X(\omega)| \exp\left(-j\frac{1}{4\pi}\frac{\tau}{B}\omega^2\right)\exp\left(j\frac{\pi}{4}\right)$$

$$\text{where } |X(\omega)| \approx \begin{cases} 1, -\pi B \le \omega \le \pi B \\ 0, elsewhere \end{cases} \tag{2.9}$$

The above equation (2.9) represents the frequency domain representation of the LFM signal that contains Fresnel sine and cosine integrals [1]. The above expression holds good for proper value of time-bandwidth product (for example, $\tau B > 10$). Thus, magnitude response is rectangle shaped and phase response is quadratic in nature. The spectrum of LFM signal depends on Time-Bandwidth product.

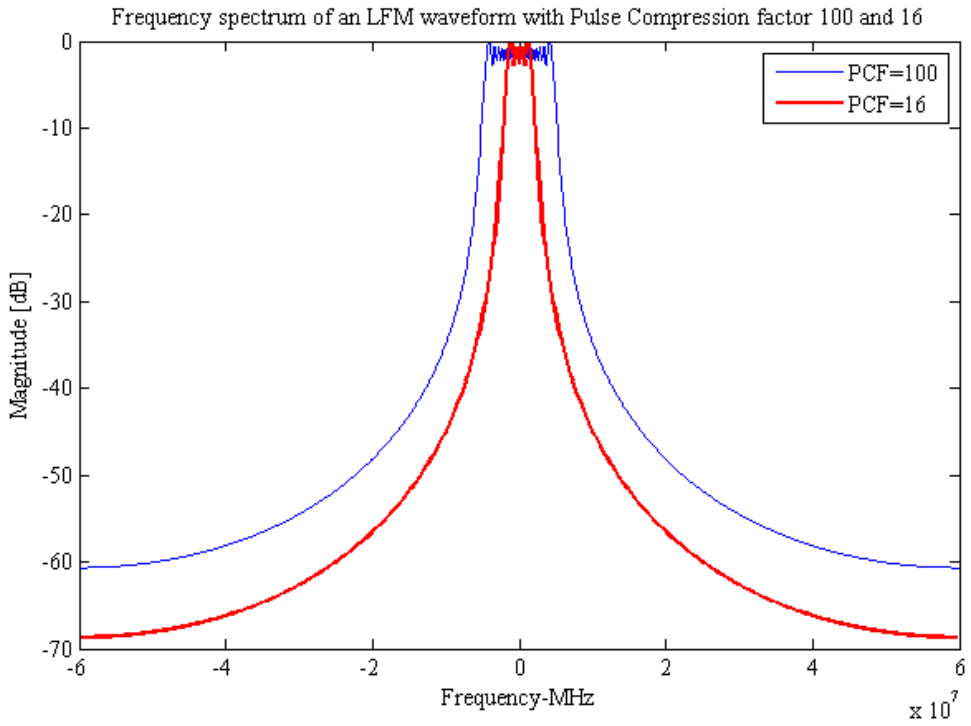

Figure 2.4. *Spectral comparisons with time-bandwidth 16 and 100*

The above Figure 2.4 represents the LFM spectrum of two waveforms with time-bandwidth product 16 and 100. The red curve represents the time-bandwidth product of 16 and blue curve represents the time-bandwidth product 100. The increase in value of time- bandwidth product spectrum has sharp transition. The frequency range $-B/2 \le f \le B/2$ shows that most of the signal energy is present in the range. For higher values of $\tau B \ge 100$, most of the energy (approx. 98% to 99%) is present in the frequency range $-B/2 \le f \le B/2$. From the above Figure 2.4 it is observed that $\pm B/2$ has a value of -6dB magnitude. The LFM waveform is doppler tolerant due to the quadratic phase term that is not found in other waveform.

The Figure 2.5 shows the simulation results of LFM signal in time domain and its frequency spectrum.

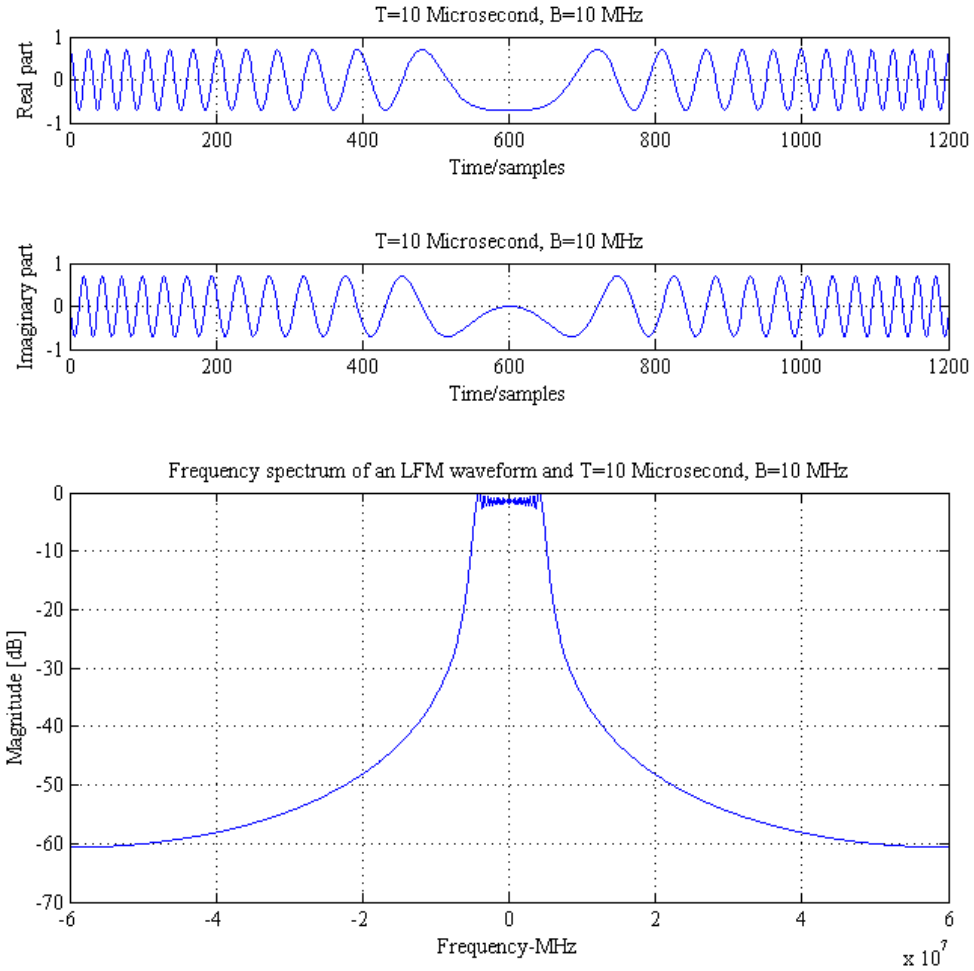

Figure 2.5. *Real and Imaginary part of LFM waveform and its frequency spectrum*

2.3. Receiver Architectures

The widely used receiver architecture in radar is superheterodyne receiver as they possess good performance. The superheterodyne receiver has disadvantage such as, cost of product is high as they require some additional components, large form factor and nonintegrable RF and IF filters [1]. The disadvantage of superheterodyne receivers is overcome by homodyne receivers. In a broadband coherent system, the homodyne receivers play an important role, also the complexity of the whole radar receiver is reduced with less bandwidth limiting components of a homodyne system. Harmonics or intermodulation products are the serious problems in receivers that cause in-band and out-of-band distortion products. These components are difficult to remove by filtering. In demodulator, in-band intermodulation is the serious problem in receivers [9].

2.3.1. Heterodyne Receivers

The received signal possesses out-of-band energy and image band signals. These components are removed by the RF front-end or preselection block of the receiver. As shown in Figure 2.6, the output of the PSF is fed to the LNA, where the noise present in

the received signal is reduced. The amplified signal is fed to the IRF, where the signal is attenuated further. The IR filter attenuates the image band frequencies and the signal is downconverted from RF to IF, with the aid of LO using mixer. The output of the mixer is fed to the IF filter. Further, the IF filter is fed to the IF amplifier. The distortion is reduced and the sufficient dynamic range is achieved in the subsequent receiver blocks. The shifting of IF to baseband and further demodulation takes place.

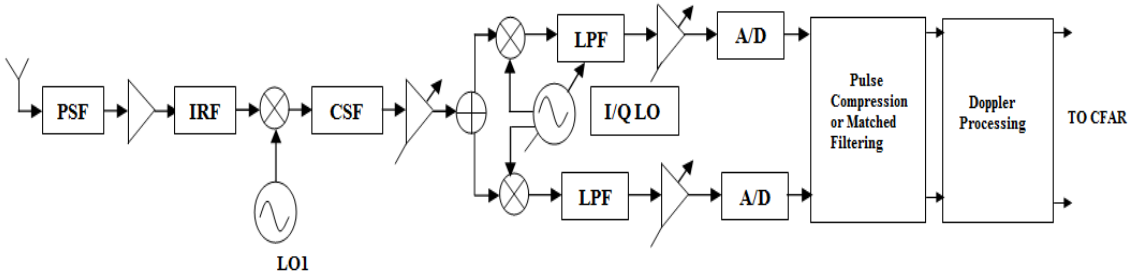

Figure 2.6. *Block Diagram of a conventional Heterodyne Receiver*

The choice of IF is a key factor in a superheterodyne receiver. Higher the value of IF, lower the necessity of IRF and attenuation of the image band becomes simple for a PSF. Thus, IR filter can be removed. If the value of IF is low, the channel select filters are selected with better quality. Thus, the choice depends on the channel selection and image rejection [17].

2.3.2. Homodyne Receivers

Homodyne receivers are also called direct conversion or zero- IF receivers, that directly downconverts RF to baseband signal with IF zero by employing low-pass filtering. By low-pass filtering the adjacent interferers are suppressed. Quadrature downconversion is employed in homodyne receivers. Homodyne receivers possess benefits over the heterodyne receivers. The homodyne receivers are not bulky, as the IF stage and IR filter is removed as shown in Figure 2.1. Channel selection and further amplification are the key functions in heterodyne receivers that are replaced by low-pass filtering and baseband amplification. Thus, monolithic integration is employed in homodyne receivers that make the receiver simple [17].

In the radar point of view, a portion of the transmitted signal from the transmitter act as a LO signal in the receiver mixer. The circulator performs the function of coupling a part of transmit signal to the receiver mixer. The circulator acts as a duplexer, so that it provides isolation between the transmitter and receiver [1]. The homodyne radar receiver is commonly employed in low-cost CW radars and FMCW radars.

The phase of the radar transmitted signal is maintained coherently. The information of the target is obtained from the phase of the received signal. The information extraction takes place at the baseband. The whole process is called the complex downconversion[9]. For a coherent technique, homodyne receiver is the most suitable configuration. But, there are certain constraints in homodyne receivers such as IQ-imbalance, D.C.

offsets, LO leakage, Intermodulation products that can be mitigated by baseband processing and quadrature phase calibration [18].

2.4. Receiver Dynamic Range

The echo signal differs each time depending upon the target. The target may be a large target or a small target. The signal strength of received signal depends on size of the target and due to $1/R^4$ (decrease in returns as a function of range). The factors affecting receiver dynamic range include the analog components of the receiver such as mixers and amplifiers and also A/D converters. In dynamic range, the lower limit represents the noise floor whereas the upper limit represents the saturation of amplifiers, mixers and other analog components. In case of radars employing linear amplifiers, upper limit of the dynamic range is the 1dB compression point. In an amplifier, the ouput in dB increases linearly as there is increase in input in dB. Thus, a straight line response is drawn, where constant slope is observed as shown in Figure 2.7 below. From the Figure 2.7, the term 1 dB compression point can be defined as the point at which there is a deviation of the output signal from the constant linear slope by 1dB.

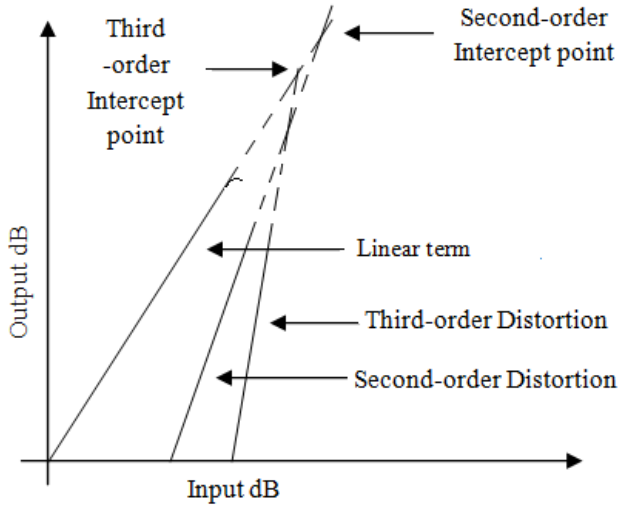

Figure 2.7. *Output signal level vs Input signal level [1]*

From the curve, it is observed that the extrapolation of second and third order distortion and also linear output results in intersection to form second and third order intercept point. In case of amplifiers, third order distortion plays a dominant role. The distortion produces different frequency components at frequencies $(2f_2 - f_1)$ and $(2f_1 - f_2)$. The intercept points are determined by combining two different signals with same input levels. The output signal has some content of distortion products. The input signal level is compared with the distortion products. Finally, the linear gain line and the distortion products are extrapolated that are measured at low signal levels [1].

The noise temperature and dynamic range of the radar receiver must be given the foremost importance in the design of mixer and amplification. For achieving dynamic range, the radar receivers must be employed with control components. For optimum

dynamic range, three dynamic range controls are implemented in radar receivers. They are MGC, AGC and STC. The echo signals from the target, on passing through the radar receiver possess a dynamic range of 120 dB or higher than the value.

3. PULSE DOPPLER RADAR

In groundbased radar, the presence of clutter in the received signal is high, as the radar beam faces towards the ground. The main source of clutter in groundbased radar is severe effect of land and sea clutter that disturbs the detection [19]. The received signal in ground-based radar depends mainly on radar-to-target geometry. The received signal has high amount of clutter due to the high PRF set to the radar. Due to the presence of clutter in the received radar signal, resolving targets becomes a tedious task, especially for the targets that are present at low altitudes. Thus, pulse doppler radars come into play for detecting low altitude or ground targets by employing doppler effects and extracting the required values [11].

The pulse doppler radar has the capability to detect received signal with small amplitude in the presence of large clutter background. In simple words, doppler radar can be defined as radars that employ doppler effect, extract the parameter by target detection. The pulse doppler radar is most suited as stationary radar, if there is a radial velocity or if there is difference in range between the radar and the target. The signal is transmitted from the radar and reflects from the target, the reflected signal is frequency shifted. Monostatic radar is considered where the transmitter and receiver are present at the same location. The distance the signal is transmitted and reflects back from the target is is called the round-trip distance. The Doppler frequency shift, measures the shifting of the reflected signal and it is calculated from the parameters such as carrier wavelength, λ that is given as $\lambda = c/f$ where c is the speed of light and f is the carrier frequency and the relative radial velocity between the radar and the target, $V_{relative}$ [10],

$$f_d = \frac{-2V_{relative}}{\lambda} \tag{3.1}$$

The negative sign in the equation (3.1) represents negative doppler shift as the target moves away from the radar. If the doppler shift is positive, the target moves towards the radar [10]. Pulse doppler radars mostly transmit the signal with high average transmitted power as they operate in high PRF. Due to the increase in average transmitted power, there is increase in SNR value, with easy detection of targets. One constraint in high PRF radar is range ambiguity, as it is difficult to detect targets that are present at long range [11].

The pulse doppler radar finds its wide application in automotive sector. Earlier, the vehicles use ultrasonic sensors and cameras to detect the vehicles in blind spot. As the ultrasonics and the cameras has disadvantage in fog and rain, pulse doppler radars are widely used at present in automotive safety systems [20].

3.1. Configuration of Pulse Doppler Radar

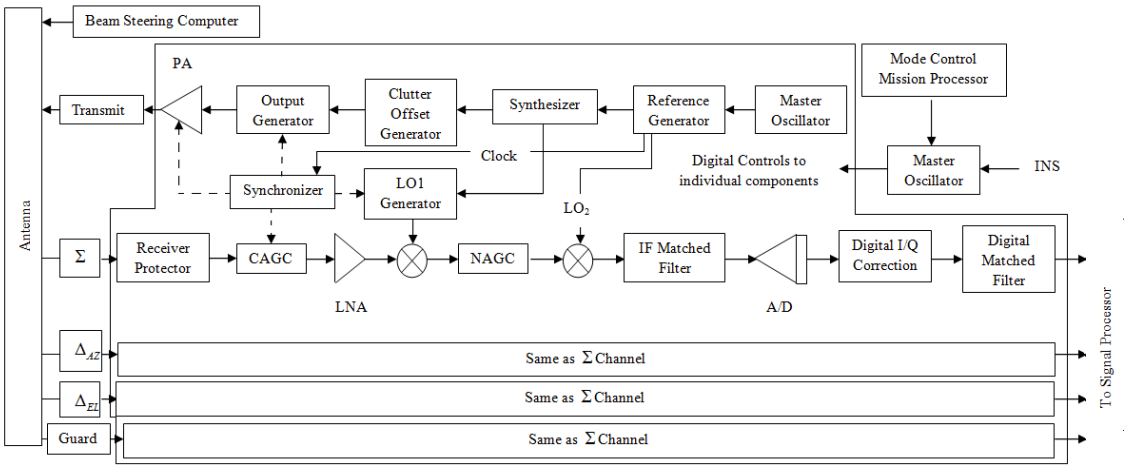

Figure 3.1. *Block diagram of pulse doppler radar transceivers [10]*

The Figure 3.1. shows the block diagram of pulse doppler radar transceivers. The control processor controls the overall radar functioning. The control processor receives the input from the INS and the control processor is operated by Mode Control Mission Processor. The pulse doppler radars employs coherent signal processing technique where the phase is assumed to same from pulse to pulse. Pulses with coherency are capable of providing better doppler resolution [21]. The phase of the transmitted pulse is maintained the same using LO that is phase referenced to a Master Oscillator. At baseband, output of the radar receiver produces I and Q components. The phase difference between the transmitted and received pulses can be estimated by expressing the complex signal, $(I + jQ)$ in phasor form. The received echo strength can be estimated by performing modulus operation on the complex signal $(I + jQ)$.

In the transmitter part of the pulse doppler radar as shown in Figure 3.1, the Master Oscillator generates sinusoidal signal. The output of the Master Oscillator is fed to Reference generator, where it outputs clock and part of it is fed to Synchronizer. The function of the synchronizer is to synchronize the various radar components by distributing the clocks from reference generator. The synchronizer allows transmit power to be transmitted by disabling the receiver by forming the range gates. The output of the reference generator is fed to the synthesizer, where the transmit carrier signal is generated and a part of the signal is fed to the LO1. The synthesizer is fed to the clutter offset generator, where the transmit carrier is shifted. The output generator produces the necessary RF signal to be transmitted, and the signal is further amplified by Power Amplifier and then fed to antenna. The antenna may be a single antenna that can be used commonly between the transmitter and receiver as shown in Figure 3.1 by using duplexer. Thus, by using duplexer either transmitter or receiver can be switched for transmitting or receiving pulse. The antenna can be operated electrically or manually. The receiver protector protects the receiver by preventing the receiver from burning out from the transmitter output. The function of CAGC is to prevent leakage from the transmitter to the receiver

so that the receiver do not saturate. The function of NAGC is to prevent the thermal noise so as to enhance the dynamic range of the receiver. In the digital pre-processing stage, the superheterodyne or direct-conversion receivers are employed to convert RF signal to baseband. Thus, complex downconversion is employed in the receivers for generating I and Q signals. The real, I and imaginary, Q part of the complex signal is passed through the post-processing unit to extract the information about the target.Thus, in the receiver after the baseband signal processing, the mainbeam clutter of the received signal is shifted to DC. Other than the clutter at DC, the non-linearities caused by power amplifiers and intermodulation caused due to mixer and video harmonics that falls near DC can be filtered with the mainbeam clutter.

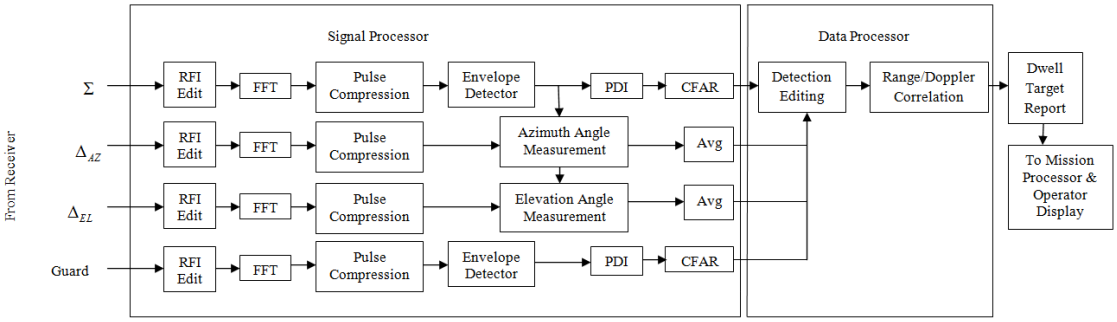

Figure 3.2. *Post Processing in pulse doppler radar [10]*

As shown Figure 3.2. the main post processing block in pulse doppler radar is doppler processing, where the SCR is improved by filtering main beam clutter using doppler filter bank. Before the doppler processing, the received radar signal has a presence of RFI that can be detected before coherent detection. Generally, FFT is applied in doppler filter bank. If the number of filters is less, DFT can be implemented to the filter bank. Pulse compression or matched filtering is a technique, for decreasing the pulsewidth, by reducing the sidelobe levels of the signal using proper weights. By reducing the sidelobe levels, it is easy to resolve the targets.

After pulse compression and doppler filtering, the envelope detector outputs a signal of the form $\sqrt{I^2+Q^2}$. The generally used detectors are linear detectors as they maintain the dynamic range of the signal by using fixed point processors. After envelope detection, the output of envelope detector is passed through the PDI.The PDI sums up the output of range gate doppler filter. The $\sum$ -channel in the radar has a presence of range-doppler cell, where output of PDI is compared with a threshold by CFAR. If the amplitude is greater than threshold, it is said to be detection. CA-CFAR algorithm is widely used CFAR algorithm. Thus, the interference is detected by varying the thresholds dynamically. The CFAR is implemented using DSPs or FPGAs. Currently, the CFAR algorithm is implemented using GPU in pulse doppler radar [22]. FPGA based softcore

architecture is one of the efficient method of implementation that provides highest processing requirements [23].

The azimuth and elevation angles of the target are recorded in the corresponding channels Δ_{AZ} and Δ_{EL}. To estimate the elevation and azimuth angles, the ratio of $\Delta_{AZ}/\sum$ and $\Delta_{EL}/\sum$ is calculated and the imaginary part is considered for the corresponding range-doppler cells. The final step in radar processing is to display the target with the proper range, velocity and angle measurements of the target. The whole processor is carried out by mission processor with accuracy [10].

The range of the target can be estimated from the expression [24],

$$R = \frac{c\Delta t}{2} \text{ where } c = \frac{c_0}{\sqrt{\varepsilon_r}} \tag{3.2}$$

The range can be estimated, if the velocity of electromagnetic wave c and time the electromagnetic wave travels between the target and the radar Δt is known. For estimating the velocity of an electromagnetic wave, the speed of light in vacuum c_0 and relative permittivity ε_r must be known. The relative velocity of the target from the radar system can be estimated from the doppler shift of the received signal, f_d and centre frequency f_0. The doppler shift is given as the difference between the doppler frequency and centre frequency, $f_d = f_t - f_0$. The relative velocity is given as [24],

$$v_r = \frac{cf_d}{2f_0} \text{ So } v \ll c \tag{3.3}$$

The Doppler shift can be defined as, shifting of frequency from the centre frequency due to the presence of target with respect to signal source. If the movement of target is towards the signal source it is called the positive doppler shift. If the movement of target is away from radar, it is called the negative doppler shift.

The below Figure 3.3 shows the transmitted and received pulses of a pulsed radar system. From the Figure 3.3, it is possible to estimate maximum unambiguous range, $R_{\max}$ [24],

$$R_{\max} = \frac{cT_p}{2} \tag{3.4}$$

Where c is the velocity of light and T_p is the PRT. Maximum unambiguous range can be defined as, the maximum distance that a pulse could travel from the transmitter to the receiver, before emitting the next pulse. If the range exceeds the unambiguous range, ghosts targets are formed as shown in Figure 3.3. If the echo signal of the first pulse is received after the second pulse is transmitted, the range is wrongly calculated by the radar as $T_p + \Delta t_3$. In pulse radar, range resolution depends on pulse width, τ_P [24].

$$\delta_r = \frac{c\tau_P}{2} \approx \frac{c}{2B} \tag{3.5}$$

Proper resolution can be obtained, if received echo signals do not overlap. From the above equation (3.5), if the pulse bandwidth decreases, the range resolution decreases and vice versa. Thus, range resolution is directly proportional to pulse bandwidth [24].

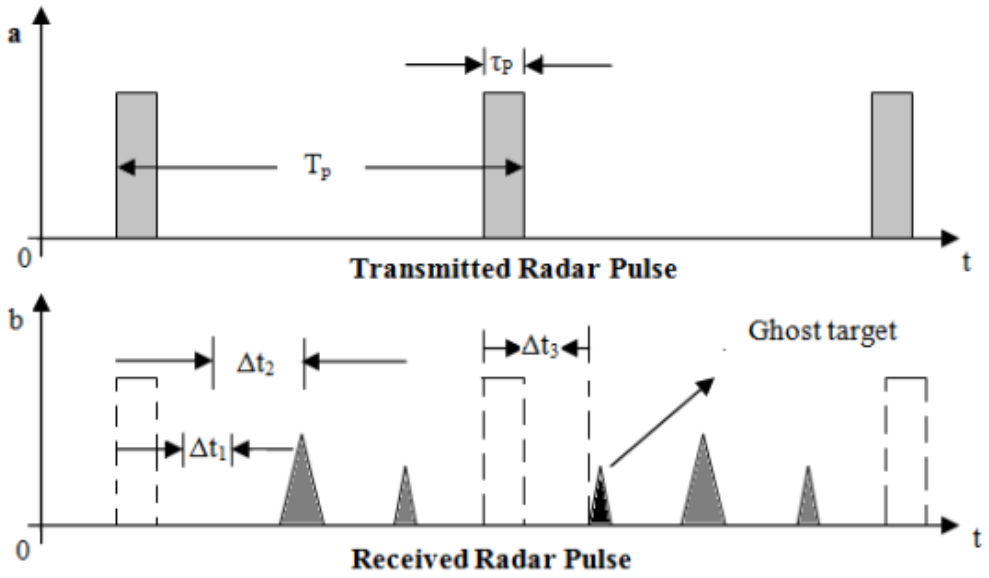

Figure 3.3. *Transmitted and received pulse doppler radar signals [24]*

3.2. Doppler Spectrum

In radar, the coherent detector output in receiver contains the information about the stationary targets and clutter, noise from the receiver, non-linearities due to the power amplifier and mixer, noise due to the atmosphere and galactic sources, jammer signals and electromagnetic interferences due to communication signals. As the target is stationary or moving, the received signal may contain several contributions from different sources. Thus, it is necessary to analyse the doppler spectrum for the corresponding range bin. For the corresponding range bin, DTFT of data is taken from multiple pulses. The final doppler spectrum has several contributions from different signal sources.

The analysis of the doppler spectrum can be explained with further illustration with stationary coherent radar. The stationary coherent radar transmits a signal where it hits a target and the received signal is received in the particular range bin where the signal has a presence of three targets in motion in which the two targets possess negative doppler shift and one target with positive doppler shift. The doppler spectrum as shown in Figure 3.4 is plotted only till $\pm PRF/2$, as the remaining samples repeat the same portion that is present outside $\pm PRF/2$. From the Figure 3.4 it is seen that, around zero doppler shift, presence of clutter is detected due to the presence of trees and grass as they are stationary. If the clutter is moving, there is a doppler spread in the spectrum. The doppler spread in the clutter depends on the type of clutter and weather. The other reason for doppler spread in clutter depends on traffic due to the vehicles and air conditioning fans that leads to the spread in the clutter [1].

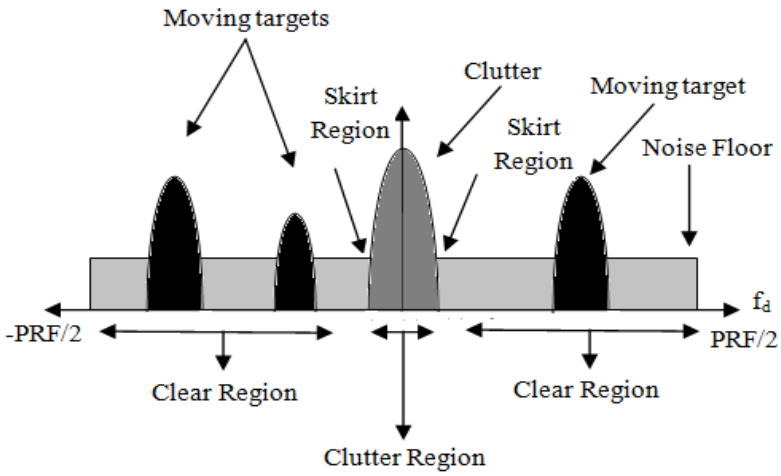

Figure 3.4. *Doppler spectrum for the corresponding range bin [1]*

From the doppler spectrum as shown Figure 3.4 shows the doppler spectrum with three notches, with one target in positive doppler shift and the remaining two targets in negative doppler shifts. The position of targets on the doppler axis depends upon the radial velocity of each target. As indicated in the Figure 3.4 the doppler shift lies in between the interval $(-PRF/2, +PRF/2)$, if the radial velocity lies between the intervals $(-\lambda.PRF/4, +\lambda.PRF/4)$. The clutter amplitude is computed from CNR Ratio. The CNR Ratio is obtained from radar range equation where the target RCS is substituted by total RCS. In the Figure 3.4 the Doppler region that is free from clutter is called the clear region. Noise is distributed uniformly all over the Doppler shift. The clutter region is the region in which the interference is higher than the noise. There is a transition between the clutter and noise where the clutter and noise are equal called the transition region.

In radar, the information about the target and clutter are stored in range bins. The presence of clutter is distributed over the range bins as the clutter strength varies according to the terrain. The presence of noise in the spectrum is distributed at all ranges and doppler shifts uniformly. The Figure 3.5 shows that the targets, clutter and noise are distributed over range and doppler. The targets are present at different range bins and the clutter is present at all range bins at zero Doppler shifts [1].

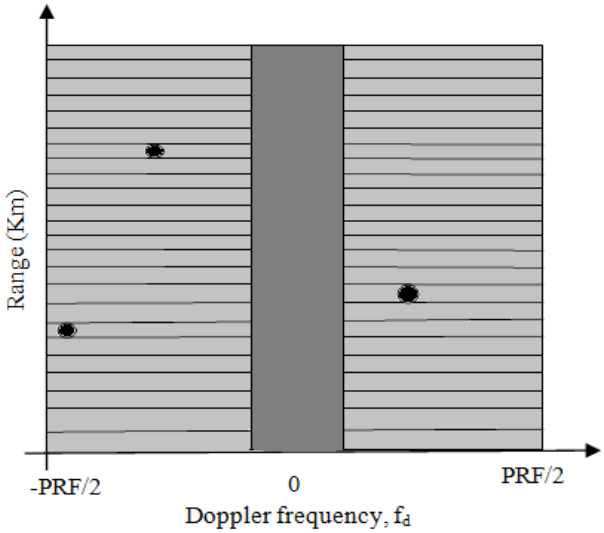

Figure 3.5. *Range-Doppler spectrum [1]*

Consider 10GHz radar where the range- velocity spectrum is plotted as shown in Figure 3.6 in which the plot is 3D- plot. The axis of the 3D plot represents power, range and velocity. From the Figure 3.6 it is observed that at zero velocity, presence of clutter is detected and three targets are detected that is present above the noise floor. The right part of the Figure 3.6 shows the contour plot that is easy to represent the target and the clutter, where the axis is range and veloctity and the noise floor is not shown in the plot. The doppler spectrum can be plotted using appropriate window functions such as hamming window to reduce the doppler sidelobes [1].

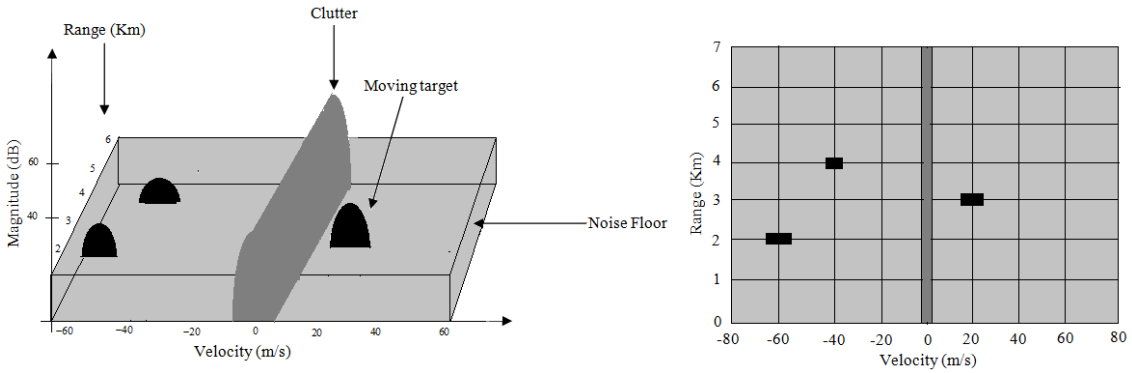

Figure 3.6. *3D plot and contour plot of Range- Doppler spectrum [1]*

3.3. Range Gating

Range gating is a concept, where the transmit pulses are divided equally into multiple cells called the range gates. The advantage of implementing range gate concept in radar is to remove noise and clutter so that the desired target signal is not affected and also the target can be tracked with ease and range measurement becomes simple. For example, surveillance radar is considered, the range gates are designed such that the radar could detect the targets within the interpulse period at any range. Some special cases include $\tau_t = \tau_g$ and $\tau_g > \tau_s$ where τ_t is the transmit pulse width, τ_g is the gate width and τ_s is the

gate spacing.The first case $\tau_t = \tau_g$, where the SNR is maximum, that leads to good performance of the radar with good resolution. The second case, $\tau_g > \tau_s$, reduces the range gate straddle loss [10].

Straddle loss in radar is a type of loss in radar, due to the successive placement of FFT filter resulting in falling of targets doppler value between the each FFT filter. Straddle loss results in loss in power of the target doppler signal, where the loss can be analyzed using the FFT filter response. The straddle loss can be compensated by reducing the frequency separation between the consecutive doppler filters, so that the overlap between the frequency responses of each doppler filters is less. This could be achieved by adding zero-padded inputs to the doppler filter [25].

3.4. Ambiguities and PRF Selection

PRF is an important characteristic of pulsed radar system. The measure of time between the start of the first pulse to the start of the next pulse is called the PRT and the inverse of PRT is the PRF [26]. Doppler resolution is a key parameter in pulse doppler radar. Better doppler resolution is obtained by uniform spacing of coherent pulses. Thus, pulses are transmitted coherently with good autocorrelation properties at certain PRF. The received echoes are processed coherently at the receiver part. This causes large ambiguities in matched filter delay doppler response in delay axis of PRT and along the doppler axis at multiple PRF. Decreasing the PRF may be a possibility of reducing the ambiguity but affects the doppler resolution. Thus, pulse doppler radars are classified based on PRF [21]. They are low PRF, medium PRF and high PRF radars.

The low PRF radar is a type of radar in which the radar is doppler ambiguous but the range is unambiguous with accurate range measurements. Medium PRF radar is both range and doppler ambiguous but provides a better average transmitter power compared to low PRF radar. A high PRF radar is range ambiguous and doppler unambiguous. A pulse doppler radar is high PRF radar as they provide high average transmitted power with better clutter rejection [11]. In a high PRF radar, the presence of clutter in received echo is obtained at a distance greater than the unambiguous range, foldover occurs so that the spectrum of longer ranges are aliased on specrum of shorter ranges, that is a common problem in high PRF radar [1]. Some pulse doppler radars employ Medium PRF. Pulse doppler radar employing a medium PRF may lead to formation of blind regions and ambiguities in range and doppler of target returns. Thus, it is necessary for medium PRF radar to have more than one PRF as the range and doppler are ambiguous. For this case, simulated annealing algorithm plays an important role in choosing the optimum value of PRF in medium PRF radar [27]. Most of the radars use multiple PRF as discussed in the below sections to improve the ambiguity resolution. Other than the simulated annealing algorithm, other adaptive genetic algorithms are implemented to improve the ambiguity resolution [28].

3.4.1. Range Ambiguity

Pulse doppler radar that uses high PRF pulse streams generally experiences range ambiguity. To resolve range ambiguity multiple high PRFs pulse streams are sent in each processing interval. The range ambiguity can be resolved by considering two PRFs f_{r_1} and f_{r_2} with unambiguous ranges R_{u1} and R_{u2} . It is to be noted that [11],

$$R_u \gg R_{u1}R_{u2} \tag{3.6}$$

From the equation (3.6), the desired unambiguous range R_u is greater than the radar unambiguous ranges. Let f_{rd} be the desired PRF for the desired unambiguous range R_u . The desired PRF can be found by coincidence of transmit PRF1 and PRF2 as shown in Figure 3.7 The values for PRF are set as $f_{r_1} = Nf_{rd}$ and $f_{r_2} = (N+1)f_{rd}$ or $f_{r_1} = (N+1)f_{rd}$ and $f_{r_2} = Nf_{rd}$ where N is an integer. The true target location can be found by, coincidence of received pulse from PRF1 and PRF2. The desired unambiguous range can be estimated from desired time delay $(T_d = 1/f_{rd})$. For PRF1 and PRF2, the corresponding time delay for the receive pulses is represented as t_1 and t_2. Let M_1 denote the number of PRF1 intervals between transmit and received signal with respect to true target location. For PRF2, M_2 is similar to that of M_1 . The possibilities are $M_1 = M_2 = M$ or $M_1 + 1 = M_2$ at an interval 0 to T_d . Thus, radar measures t_1 and t_2 .The analysis is carried out as three cases as $t_1 < t_2$, $t_1 > t_2$ and $t_1 = t_2$.

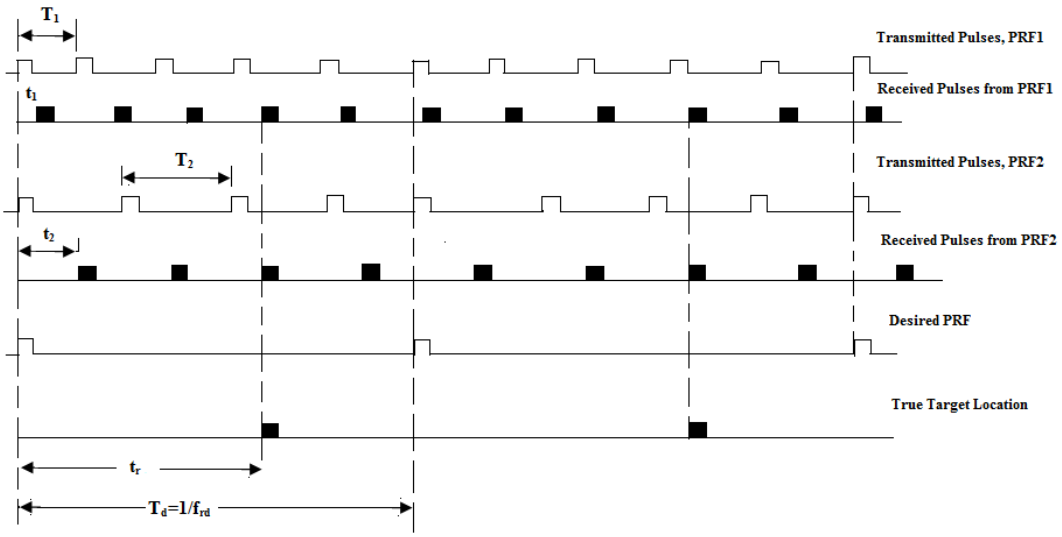

Figure 3.7. *Range ambiguity resolution [11]*

Consider the case $t_1 < t_2$,

$$t_1 + \frac{M}{f_{r_1}} = t_2 + \frac{M}{f_{r_2}} \tag{3.7}$$

On solving above equation (3.7) we get [11],

$$M = \frac{t_2 - t_1}{T_1 - T_2} \tag{3.8}$$

Where $T_1 = \frac{1}{f_{r_1}}$ and $T_2 = \frac{1}{f_{r_2}}$. The roundtrip time t_r can calculated with respect to true target location, is given as,

$$t_r = MT_1 + t_1 \tag{3.9}$$

$$t_r = MT_2 + t_2 \tag{3.10}$$

The true target range is given as,

$$R = \frac{ct_r}{2} \tag{3.11}$$

Consider the case $t_1 > t_2$,

$$t_1 + \frac{M}{f_{r_1}} = t_2 + \frac{M+1}{f_{r_2}} \tag{3.12}$$

On solving above equation (3.12) we get [11],

$$M = \frac{(t_2 - t_1) + T_2}{T_1 - T_2} \tag{3.13}$$

The roundtrip time t_r can calculated with respect to true target location, is given as,

$$t_{r_1} = MT_1 + t_1 \tag{3.14}$$

The true target range is given as,

$$R = \frac{ct_{r_1}}{2} \tag{3.15}$$

Consider the case $t_1 = t_2$. The round trip time is,

$$t_{r_2} = t_1 = t_2 \tag{3.16}$$

and the true target range is given as [11],

$$R = \frac{ct_{r_2}}{2} \tag{3.17}$$

Blind range problem can be resolved by introducing third PRF signal. The minimum range that the radar could detect target is the blind range. The three Pulse Repetition Frequency (PRF) can be set as $f_{r_1} = N(N+1) f_{rd}$, $f_{r_2} = N(N+2) f_{rd}$ and $f_{r_3} = (N+1)(N+2) f_{rd}$

3.4.2. Doppler Ambiguity

The doppler ambiguity can be explained for the pulse doppler radars that employ medium PRF. As the medium PRF technique is both range and doppler ambiguous, the doppler ambiguity has to be resolved. The range ambiguity is discussed in previous section. In the line spectrum of pulse doppler radar as shown in Figure 3.8, each pulse is repre-

sented as line separated by PRF, f_r and the envelope takes the *sinc* form. The doppler value of the target can be estimated from doppler filter bank such that the doppler shift is less than half of the bandwidth of individual filters [11].

$$f_r = 2 f_{d\max} = (2v_{r\max})/\lambda \tag{3.18}$$

where $f_{d\max}$ is the maximum value of doppler frequency, $v_{r\max}$ is the maximum radial velocity of the target, λ is the wavelength of the radar.

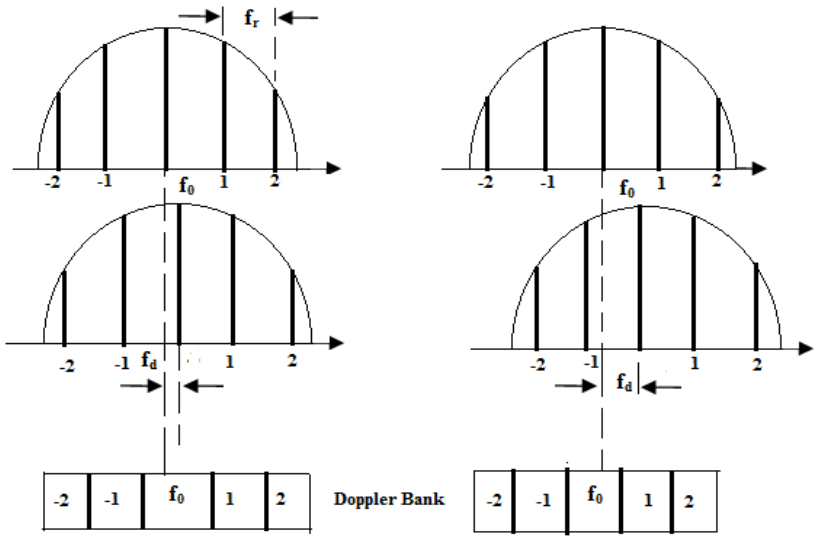

Figure 3.8. *Doppler ambiguity resolution showing transmitted & received signal [11]*

The radar is said to be doppler ambiguous, if the successive spectral lines inside the spectrum moves adjacent within the doppler spectrum. The doppler ambiguity can be resolved by using high PRF techniques for the case of high velocity targets. In a high speed targets it is not possible for the radar to be range and doppler unambiguous. The doppler ambiguity can be resolved by using multiple PRF pulses. The multiple PRF schemes can be implemented in a dwell interval or by using a single PRF in one scan and another PRF in next scan so that ambiguities can be resolved. The second technique has some disadvantage due to the change in charactersistics of the received signal each time. The analysis of doppler ambiguity is similar to that of the range ambiguity. Instead of t_1 and t_2, measure f_{d_1} and f_{d_2}. Thus, three cases are analysed. They are $f_{d_1} > f_{d_2}$, $f_{d_1} < f_{d_2}$ and $f_{d_1} = f_{d_2}$.

Consider the case $f_{d_1} > f_{d_2}$, and then M can be expressed as [11],

$$M = \frac{(f_{d_2} - f_{d_1}) + f_{r_2}}{f_{r_1} - f_{r_2}} \tag{3.19}$$

Consider the case $f_{d_1} < f_{d_2}$, and then M can be expressed as [11],

$$M = \frac{f_{d_2} - f_{d_1}}{f_{r_1} - f_{r_2}} \tag{3.20}$$

The true doppler value can be expressed of the form,

$$f_d = Mf_{r_1} + f_{d_1} \tag{3.21}$$

$$f_d = Mf_{r_2} + f_{d_2} \tag{3.22}$$

Consider the case $f_{d_1} = f_{d_2}$ [11],

$$f_d = f_{d_1} = f_{d_2} \tag{3.23}$$

Similar to the range ambiguity, there is a possibility of blind doppler that can be resolved by third PRF [11].

4. RF IMPERFECTIONS AND MODELLING

In a pulse doppler radar, the moving targets are separated from the clutter by the process called doppler processing. In doppler processing the thermal noise floor is assumed to be constant, also assume that the target radial velocity is higher than $(> 2v_{relative}/\lambda)$, where $v_{relative}$ is the relative radial velocity, with a high PRF in an unambiguous clutter spectrum, so that the clutter would be detected. The concept of coherency is an important characteristic of radar so that the phase is maintained the same for each pulse. If the coherency is lost, amplitude and phase instability occurs, that causes a spread in mainbeam clutter that would ultimately raise the noise floor. In this thesis, the effect of non-linearities is given importance than the effect of clutter. The nonlinearities in a radar receiver can create false targets due to the additional spectral signals produced that can be misunderstood as targets by the operator. The linearity and sensitivity of the radar in an environment with clutter depends on the dynamic range of the radar [10].

In the receiver point of view, the thesis deals with DCRs, there are some drawbacks in DCRs such as IQ-Imbalance, 2nd and 3rd order non-linearities, DC Offset and phase noise. These impairments affect the pulse doppler radar systems. In this chapter, the causes and effects of the non-linearities are studied. Simple mathematical expressions are modelled to demonstrate the impact of non-linear distortion in pulse doppler radar receivers.

4.1. Modelling of RF and Baseband Signal in Radar Transceiver

Before studying about the RF imperfections and modelling, it is necessary to model the RF and baseband signal in radar transceiver. To build an efficient transceiver, it is necessary to study about the bandpass signals and its associated systems. The I/Q systems play an important role in transmitter and receiver. In transmitter, upconversion takes place whereas in the receiver, downconversion takes place. The radar transmitter converts the baseband to RF-signal for transmission. Thus, two methods can be implemented. The upconversion can be implemented by using parallel real signals or by using complex signals.

The Baseband signal is given as [1],

$$x(t) = A(t)e^{j\left(\pi\frac{B}{\tau}t^2\right)} \tag{4.1}$$

The baseband signal in I-Branch and Q-Branch are given as,

$$x_I(t) = A(t)\cos\left(\pi \frac{B}{\tau} t^2\right) \tag{4.2}$$

$$x_Q(t) = A(t)\sin\left(\pi \frac{B}{\tau} t^2\right) \tag{4.3}$$

where time varying phase $\phi(t) = \pi \frac{B}{\tau} t^2$. The LO signal in I-Branch is $\cos(\omega_{LO} t)$ and the LO in Q-Branch is $\sin(\omega_{LO} t)$ as two parallel real signals are employed in I and Q branches for upconversion.

$$x_{RF1}(t) = A(t)\cos(\phi(t)) \times \cos(\omega_{LO} t) \tag{4.4}$$

$$x_{RF2}(t) = A(t)\sin(\phi(t)) \times (\sin(\omega_{LO} t)) \tag{4.5}$$

where $x_{RF1}(t)$ and $x_{RF2}(t)$ are the RF signals after upconversion.

On combining (4.4) and (4.5),

$$x_{RF}(t) = A(t)\cos(\phi(t)) \times \cos(\omega_{LO} t) - A(t)\sin(\phi(t)) \times (\sin(\omega_{LO} t)) \tag{4.6}$$

$$x_{RF}(t) = A(t)\cos\left(\omega_{LO} t + \phi(t)\right) \tag{4.7}$$

where $x_{RF}(t)$ is the transmitted signal in terms of parallel real signals.

The basic upconversion can be implemented in terms of complex signals.The LO signal is expressed in exponential form as $e^{j\omega_{LO} t}$. By complex mixing,

$$x_{RF}(t) = A(t)e^{j\phi(t)} e^{\omega_{LO} t} = x(t)e^{j(\omega_{LO} t + \phi(t))} \tag{4.8}$$

$$x_{RF}(t) = \mathrm{Re}\left[x(t)e^{j(\omega_{LO} t + \phi(t))} \right] \tag{4.9}$$

$$x_{RF}(t) = A(t)\cos(\omega_{LO} t + \phi(t)) \tag{4.10}$$

where $x_{RF}(t)$ is the transmitted signal in terms of complex signals.

In the radar receiver, the received echo signal can be expressed as [8],

$$y_{RF}(t) = A(t)\cos(2\pi f_d t + \pi \frac{B}{\tau} t^2 + \varphi_0) \tag{4.11}$$

where f_d is the doppler frequency of the target, time varying phase $\phi(t) = \pi \frac{B}{\tau} t^2$ and φ_0 is the progressing phase shift from pulse-to-pulse due to doppler shift. On applying complex downconversion to the received signal,

$$y_{RF}(t) = \mathrm{Re}\left[x(t)e^{j(\omega_d t + \varphi_0)} \right] e^{-j\omega_{LO} t} \tag{4.12}$$

where $e^{-j\omega_{LO} t}$ is the complex exponential to obtain the baseband signal as shown Figure 4.1. On simplifying (4.12) the baseband signal is,

$$y(t) = A(t)\,\mathrm{e}^{(j(\omega_a t + \phi(t) + \varphi_0))} \tag{4.13}$$

where $\omega_a = \omega_d - \omega_{LO}$

Thus, equation (4.13) shows the baseband signal with the effect of doppler [8].

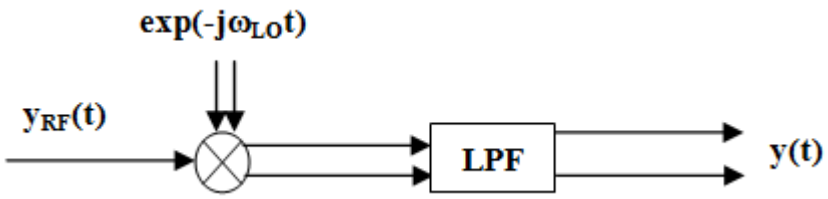

Figure 4.1. *I/Q Downconversion using complex signals [5,7]*

4.2. I/Q Imbalance

The radar using DCR is better than superheterodyne receivers because they are not bulky and power consumption is reduced. They also provide good attenuation to image bands and remove the need for analog filtering for rejecting image band. But, there is some imbalance in I and Q branches in both amplitude and phase. Eventhough the quadrature downconversion introduces frequency translation, the imbalances introduce additional frequency translation so that the resultant signal would be the mixture of image bands and desired signals. In a DCR, with careful analog design the minimum achievable phase imbalance $1-2^{\circ}$ and amplitude imbalance would be $1-2\%$ [6, 8].

The effect of IQ- Imbalance in a pulse doppler radar introduces false targets that would mask the real target at a negative doppler frequency [8]. Generally in IQ- Imbalance, the phase of the I-part must lead the Q-part for a positive doppler. In a radar receiver, if the LO frequency is higher than RF frequency, the doppler frequency gets inverted. Careful design of receiver is important. The IQ-Imbalance can be corrected by implementing compensation algorithms using DSPs [1]. Direct digital coherent detection is mostly implemented in radar as it reduces IQ-imbalance due to physical components so that it reduces the effect of amplitude and phase imbalance in a radar and calibration that is required in analog coherent detection. The amplitude and phase imbalance generates some spurious components on the desired signal (with clutter) at image frequency. By using doppler filter, clutter can be filtered out. If the clutter is present at the zero doppler, the presence of spurious signals would be present at zero doppler. Thus, the effect of amplitude and phase imbalance would be zero at stationary clutter [12].

The modelling of IQ imbalance can be illustrated by considering an RF signal [8],

$$z_{RF}(t) = \cos(2\pi f_{RF} t) \tag{4.14}$$

The Local Oscillator $u(t)$ is used in quadrature downconversion with amplitude imbalance of $g = 1+\varepsilon$ and phase imbalance of ϕ as expressed in the equation (4.18) below,

$$u(t) = \cos(2\pi f_{LO} t) - j.(1+\varepsilon)\sin(2\pi f_{LO} t + \phi) \tag{4.15}$$

By multiplying equation (4.14) and (4.15) and low pass filtering, I and Q components of baseband can be recovered by using the expression $f_{IF} = f_{RF} - f_{LO}$

$$x_I(t) = \frac{1}{2}\cos(2\pi f_{IF} t) + D_I \tag{4.16}$$

$$x_Q(t) = \frac{g}{2}\sin(2\pi f_{IF} t - \phi) + D_Q \tag{4.17}$$

$$x(t) = \frac{1}{2}\cos(2\pi f_{IF}t) + j\frac{g}{2}\sin(2\pi f_{IF}t - \phi) + D_{IQ} \tag{4.18}$$

$$x(t) = \frac{1}{4}\left[e^{j2\pi f_{IF}t}(1 + g.e^{-j\phi}) + e^{-j2\pi f_{IF}t}(1 - g.e^{-j\phi}) \right] + D_{IQ} \tag{4.19}$$

From the above equation (4.19), it is seen that, the result would be the mirror image that is superimposed on the desired complex signal. Additionally, there is a presence of DC offset in I and Q signal. The appropriate weights of the signal can be represented as K_1 and K_2 and the equation (4.19) can be rewritten as [8],

$$x(t) = K_1.e^{j2\pi f_{IF}t} + K_2 e^{-j2\pi f_{IF}t} = K_1.z(t) + K_2.z^*(t) \tag{4.20}$$

where $K_1 = \frac{(1 + g.e^{-j\varphi})}{4}$ and $K_2 = \frac{(1 - g.e^{j\varphi})}{4}$

4.3. Intermodulation Distortion

Intermodulation distortion is an RF imperfection in radar that is due to the linear combination of fundamental frequencies. Intermodulation distortion is one of the non-linearity in DCRs. The intermodulation distortion can be classified as second order and third order distortion. The receiver performance can be estimated using second and third order intercept points. The second and third intercept can be estimated by extrapolating the linear output curve with second and third order distortion curve. For Second order intermodulation, the fundamental frequencies f_1 and f_2 on linear combination generate products at frequencies *0, f_1-f_2, f_1+f_2, 2 f_1* and *2f_2*. For the case of third order distortion, the fundamental frequencies f_1 and f_2 on linear combination produces *2f_1-f_2, 2f_2-f_1, 2f_1+f_2, f_1+2f_2, 3f_1 and 3f_2*. In a narrowband signal, the third order distortion products are *2f_1-f_2, 2f_2-f_1* affects the spectrum of the desired signal. Thus, third order distortion is an important case. The power levels of the products that are obtained as a result of third order intermodulation products is given as [10],

$$P_{2f_1 - f_2}(dBm) = 2P_{f_1}(dBm) + P_{f_2} - 2P_{IP}(dBm) \tag{4.21}$$

$$P_{2f_2 - f_1}(dBm) = P_{f_1}(dBm) + 2P_{f_2} - 2P_{IP}(dBm) \tag{4.22}$$

The terms P_{f_1} and P_{f_2} are the input power levels at fundamental frequencies f_1 and f_2 expressed in dBm and P_{IP} is the power level of third order intercept point.

In radar, the intermodulation distortion increases the doppler width of the clutter that results in masking of the targets. False targets are generated, that are present outside the desired spectrum affect the desired signal. The desired signal that is affected due to the non-linearities can be compensated by highly sophisticated DSP techniques.

Cross-modulation distortion is a special case of intermodulation distortion where the unwanted interference signal is modulated with a RF bandwidth that is present outside the desired signal bandwidth, inturn affects the desired signal bandwidth. Due to the out-of-band interference, clutter and targets are modulated, that results in poor cancellation of clutter and side lobe performance becomes weak [10].

The basic polynomial model for the analysis of non-linear distortion is assumed to be memoryless and the expression is given as [5, 7],

$$y(t) = b_1 x(t) + b_2 x^2(t) + b_3 x^3(t) + ... \tag{4.23}$$

where the terms $x(t)$ and $y(t)$ are the input and output signals [5,7]. The resultant harmonics is given as $n \times f_1$ and $m \times f_2$, that would be the linear combination of the system given in equation (4.23) with fundamental frequencies components f_1 and f_2. The intermodulation products are given as $\pm n \times f_1 \pm m \times f_2$ where n, m=1,2,3... [5].

The baseband non-linearities are more widely discussed as the thesis concentrates on baseband non-linearities. In terms of complex signal point of view, for a second order distortion in I and Q branches, the resultant signal is given as [5, 7],

$$y(t) = b_1 x_I(t) + b_2 x_I^2(t) + j\left\{b_1 x_Q(t) + b_2 x_Q^2(t)\right\} \tag{4.24}$$

The input terms in I and Q branches as obtained from the baseband signal (4.13),

$$x_I(t) = A(t)\cos\left(\omega_a t + \phi(t) + \varphi_0\right) \tag{4.25}$$

$$x_Q(t) = A(t)\sin\left(\omega_a t + \phi(t) + \varphi_0\right) \tag{4.26}$$

The equations (4.25) and (4.26) are substituted in the above equation (4.24) to obtain a second order distortion model as follows,

$$\begin{aligned} y(t) &= b_1 A(t)\exp(j(\omega_a t + \phi(t) + \varphi_0)) + \frac{1}{2}(1+j)b_2 A^2(t) \\ &+ \frac{1}{4}(1-j)b_2 A^2(t)\exp(j(2\omega_a t + 2\phi(t) + 2\varphi_0)) \\ &+ \frac{1}{4}(1-j)b_2 A^2(t)\exp(-j(2\omega_a t + 2\phi(t) + 2\varphi_0)) \end{aligned} \tag{4.27}$$

From the equation (4.27), it is to be observed that the second order distortion components are similar on both the sides of the spectrum. Thus, equation (4.27) has a target signal $b_1 A(t)\exp(j(\omega_a t + \phi(t) + \varphi_0))$, a DC component $\frac{1}{2}(1+j)b_2 A^2(t)$, one second order distortion components at $+2\omega_a$, $\frac{1}{4}(1-j)b_2 A^2(t)\exp(j(2\omega_a t + 2\phi(t) + 2\varphi_0))$ and other second order distortion component at $-2\omega_a$, $\frac{1}{4}(1-j)b_2 A^2(t)\exp(-j(2\omega_a t + 2\phi(t) + 2\varphi_0))$.

In terms of complex signal point of view, for a third order distortion in I and Q branches, the resultant signal is given as [5, 7],

$$y(t) = b_1 x_I(t) + b_3 x_I^3(t) + j\left\{b_1 x_Q(t) + b_3 x_Q^3(t)\right\} \tag{4.28}$$

On substituting equation (4.25) and (4.26) in the equation (4.28) and rearranging the terms yields the following result as,

$$y(t) = b_1 A(t)\exp(\,j(\omega_a t + \phi(t) + \varphi_0)) + \frac{3}{4} b_3 A^3(t)\exp(\,j(\omega_a t + \phi(t) + \varphi_0)) + \frac{1}{4} b_3 A^3(t)\exp(-j(3\omega_a t + 3\phi(t) + 3\varphi_0)) \quad (4.29)$$

From the equation (4.29), it is interesting to find that the third order component $+3\omega_a$ appear at the opposite side (at $-3\omega_a$) of the target signal.Thus, a spurious component called the self distortion component falls on the desired target signal. In the equation (4.29), the target signal is placed at $b_1 A(t)\exp(\,j(\omega_a t + \phi(t) + \varphi_0))$, the self-distortion component is placed at $\frac{3}{4} b_3 A^3(t)\exp(\,j(\omega_a t + \phi(t) + \varphi_0))$ and the third order component is placed at a frequency, $\frac{1}{4} b_3 A^3(t)\exp(-j(3\omega_a t + 3\phi(t) + 3\varphi_0))$ .The desired target signal is more affected by the third order distortion than the second order distortion due to the presence of self distortion component in the target signal.

Considering the case where I and Q branches are not identical.On introducing polynomial coefficients b_1, b_2 and b_3 in I-branch and g_1b_1,g_2b_2 and g_3b_3 in Q-branch to an expression for order distortion as follows [5, 7],

$$y(t) = b_1 x_I(t) + b_2 x_I^2(t) + j\left\{ g_1 b_1 x_Q(t) + g_2 b_2 x_Q^2(t) \right\} \quad (4.30)$$

On substituting equation (4.25) and (4.26) in the equation (4.30) and rearranging the terms yields the following result as,

$$y(t) = b_1 \frac{1+g_1}{2} A(t)\exp(\,j(\omega_a t + \phi(t) + \varphi_0)) + b_1 \frac{1-g_1}{2} A(t)\exp(-j(\omega_a t + \phi(t) + \varphi_0)) + \frac{1}{2}(1 + jg_2) b_2 A^2(t) + \frac{1}{4}(1 - jg_2) b_2 A^2(t)\exp(\,j(2\omega_a t + 2\phi(t) + 2\varphi_0)) + \frac{1}{4}(1 - jg_2) b_2 A^2(t)\exp(-j(2\omega_a t + 2\phi(t) + 2\varphi_0)) \quad (4.31)$$

From the equation (4.31), it is to be observed a mirror image of the target signal is obtained at $b_1 \frac{1-g_1}{2} A(t)\exp(-j(\omega_a t + \phi(t) + \varphi_0))$ and the corresponding mirror images of the frequency components are produced at $+2\omega_a$ and $-2\omega_a$. A DC component is also produced.The mirror image is produced due to the effect non-identical modelling of I and Q branches.

For the case of third order distortion [5, 7],

$$y(t) = b_1 x_I(t) + b_3 x_I^3(t) + j\left\{ g_1 b_1 x_Q(t) + g_3 b_3 x_Q^3(t) \right\} \quad (4.32)$$

Substituting the equations (4.25) and (4.26) in the equation (4.32),

$$\begin{aligned} y(t) &= b_1 \frac{1+g_1}{2} A(t)\exp(j(\omega_a t+\phi(t)+\varphi_0)) \\ &+ b_1 \frac{1-g_1}{2} A(t)\exp(-j(\omega_a t+\phi(t)+\varphi_0)) \\ &+ \frac{3}{4} b_3 \frac{1+g_3}{2} A^3(t)\exp(j(\omega_a t+\phi(t)+\varphi_0)) \\ &+ b_3 \frac{1-g_3}{2} A^3(t)\exp(-j(\omega_a t+\phi(t)+\varphi_0)) \\ &+ \frac{1}{4} b_3 \frac{1-g_3}{2} A^3(t)\exp(j(3\omega_a t+3\phi(t)+3\varphi_0)) \\ &+ b_3 \frac{1+g_3}{2} A^3(t)\exp(-j(3\omega_a t+3\phi(t)+3\varphi_0)) \end{aligned} \tag{4.33}$$

The above equation (4.33) is a severe case compared to the previous case of non-linearities. Thus, a mirror image of the target signal, $b_1 \frac{1+g_1}{2} A(t)\exp(j(\omega_a t+\phi(t)+\varphi_0))$ is produced at $b_1 \frac{1-g_1}{2} A(t)\exp(-j(\omega_a t+\phi(t)+\varphi_0))$ and self distortion component in the target signal $\frac{3}{4} b_3 \frac{1+g_3}{2} A^3(t)\exp(j(\omega_a t+\phi(t)+\varphi_0))$ falls at $b_3 \frac{1-g_3}{2} A^3(t)\exp(-j(\omega_a t+\phi(t)+\varphi_0))$, also mirror image of the third order component at $-3\omega_a$, $b_3 \frac{1+g_3}{2} A^3(t)\exp(-j(3\omega_a t+3\phi(t)+3\varphi_0))$ falls at $+3\omega_a$, $\frac{1}{4} b_3 \frac{1-g_3}{2} A^3(t)\exp(j(3\omega_a t+3\phi(t)+3\varphi_0))$.

4.4. DC Offset

DC Offset is a major RF imperfection in a direct conversion radar receiver. The presence of DC Offset in the baseband portion of the radar receiver causes severe effects [29]. The reason for the DC Offset is due to the LO leakage. The reason for LO leakage is due to the improper isolation between the LO port and mixer input [17].

In radar receiver, the output of the A/D converter has the presence of DC offset by distorting the small signals and the receiver noise. This undesired effect can be suppressed by doppler filtering. The DC Offset can be compensated by applying proper correction algorithms at the output of the A/D converter and the correction can be implemented by including a D/A converter as shown in Figure 4.2. The compensation of DC offset can be implemented in digital domain, if the effect of DC offset is not large at the input of the A/D Converter. But this implementation causes reduction in dynamic range [10].

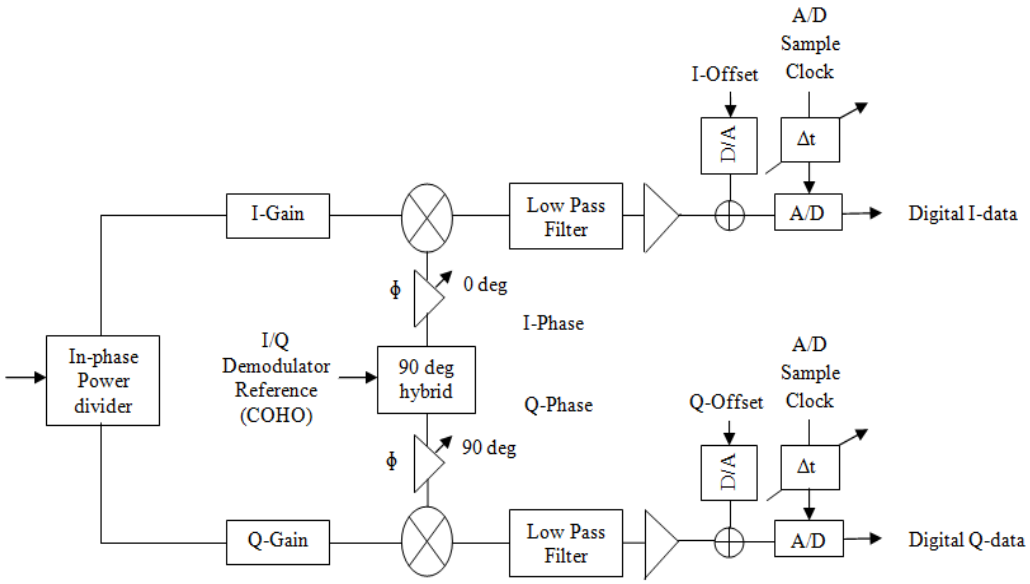

Figure 4.2. *I/Q Demodulator showing the correction of DC Offset [10]*

4.5. Phase Noise

The weak targets are masked due to the presence of phase noise in the radar signal. Thus, total noise level is the sum of thermal noise level and with a small increase in noise level that affects the radar sensitivity [10]. The phase noise decreases the SNR where the resolution of the target decreases [30].

The generation of phase noise is due to the time domain instabilities. The time domain representation of phase noise is called the jitter. In frequency domain, the sidebands get widened and the power is spread over to adjacent frequencies decreasing SNR. Phase noise is random fluctuations in phase of the signal. If the signal fluctuates randomly, it can be observed that the sidebands would gradually move downwards from the signal. The non-random fluctuations generate undesired components called spurs that causes phase variations. Phase noise is mostly related to the non-idealities of an oscillator that results in carrier frequency offset and phase offset. The phase noise is said to be more complex form of non-ideality in oscillators as the phase noise is time varying [31]. At closer frequency offset, the effect of phase noise is higher.The STALO and COHO are the two oscillators used in radar. If instabilities in these two local oscillators, the effects of phase impairments will be higher, that decreases SNR.

The effect of phase noise is higher in MTI radars. In this type of radar, the target is said to be moving and produces required doppler shift. The magnitude of target is less than the clutter, as clutter returns are assumed to be stationary (mountains, trees, etc.). The clutter portion in the spectrum can be filtered and the target signal can be examined. The clutter filtering cannot remove the noise on the clutter. The signal transmitted should have good noise performance for the radar operation [30].

5. SIMULATION PLATFORM AND OBTAINED RESULTS

In this chapter, the simulation results for the effect of non-linearities in radar receiver are illustrated. The simulations results are obtained using Matlab.The DCR are prone to non-linearities such as I/Q imbalance, non-linear distortion that includes second and third order distortion, DC offset and phase noise. In general, the effect of third order distortion on the radar receiver is atmost given importance as the third order products are closer to the desired signal. The third order products can be removed by highly sophisticated DSP techniques. In some cases second order products can be removed by simple filtering techniques. The whole simulation is carried out at baseband. The baseband non-linearities of a radar receiver are simulated. Baseband non-linearities are due to the non-linearities that take place during I/Q processing, like I/Q mixer. Finally the non-linearities are analyzed in post-processing blocks such as matched filtering and doppler processing. To illustrate the effect of non-linearities in radar receivers the following parameters are considered:

Table 5.1. *Simulation parameters*

Parameters	***Values***
Number of Pulses, NOP	100
Bandwidth of LFM,B	10MHz
Pulsewidth (Duration of transmitting pulse)	10 μs
Pulse Repetition Time, PRT	50μs
A/D Sampling Frequency, f_s	120MHz
SNR of received pulse	70dB
Normalized Doppler Frequency	0.2×pi
Amplitude of moving target	0.7

The simulation is carried out in a way such that, firstly the ideal case (without non-linearities) are simulated, then the third order and second non-linearities are modelled with some special case are simulated and analyzed.

5.1. Signal Generation

To illustrate the ideal case, I and Q signals are generated with 100 coherent pulses for processing inside the doppler filter bank. The I and Q- signals are sampled at frequency of 120MHz by A/D. For the complex signal to be pulse compressed, a pulse compression factor of 100 is obtained by the product of bandwidth and pulsewidth. The band-

width of LFM signal is 10 MHz and pulsewidth of 10 μs as shown in table 5.1. The PRT is chosen to be 50μs that is the start of the first pulse to the start of second pulse. From the value of pulsewidth and PRT, the value of delay between each pulse can be estimated. The SNR has to be high in radar so that the range resolution would be improved. Thus a SNR value of 70dB is chosen. The target is placed at 0.2 times the PRF. The value 0.2×pi is the normalized value of doppler frequency. The chirp amplitude or the amplitude of the moving target is 0.7 as illustrated in the table 5.1. On simulating with the above parameters, the complex signal is obtained as shown in Figure 5.1.

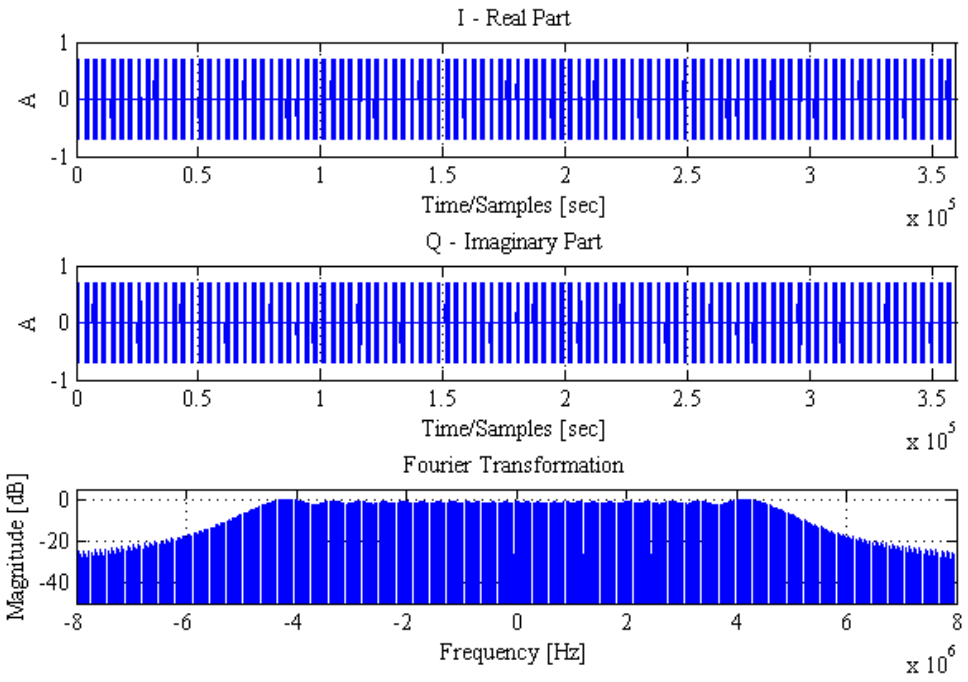

Figure 5.1. *Signal generation and pulse trail generation*

The single pulse LFM is shown in Figure 2.5. From the Figure 5.1, as the pulse compression factor increases, the frequency spectrum of the LFM signal is more rectangular in shape [1]. The desired portion of the signal is present between $(-5 \le f \le 5)$ MHz. Two sided frequency domain plot is used for constructing the frequency spectrum as it easy to analyse in baseband. The received echo strength and phase of the complex signal (I+jQ) = (0.7+j0.7) can be computed as shown in equations (5.1) and (5.2),
Received echo strength [1],

$$A = \sqrt{I^2 + Q^2} = 0.989 \tag{5.1}$$

Phase difference between the transmitted and received pulses [1],

$$\theta = \tan^{-1}\left(\frac{Q}{I}\right) = 45° \tag{5.2}$$

5.2. Matched Filtering

In matched filtering, the received signal is compared with the reference signal. The reference signal is the complex conjugate of the transmitted signal multiplied with the hamming weight function. The purpose of using weighting function is to suppress the sidelobes by introducing a mismatch between the received signals and transmit waveform. Higher the weighting causes degraded resolution due to reduction in bandwidth and loss in processing gain with a loss in SNR. Thus, a correlation operation is performed to generate the reference signal. The convolution operation is performed between the received complex signal and the reference signal. The obtained matched filtered output is similar to that of the sinc function as shown in Figure 5.2.

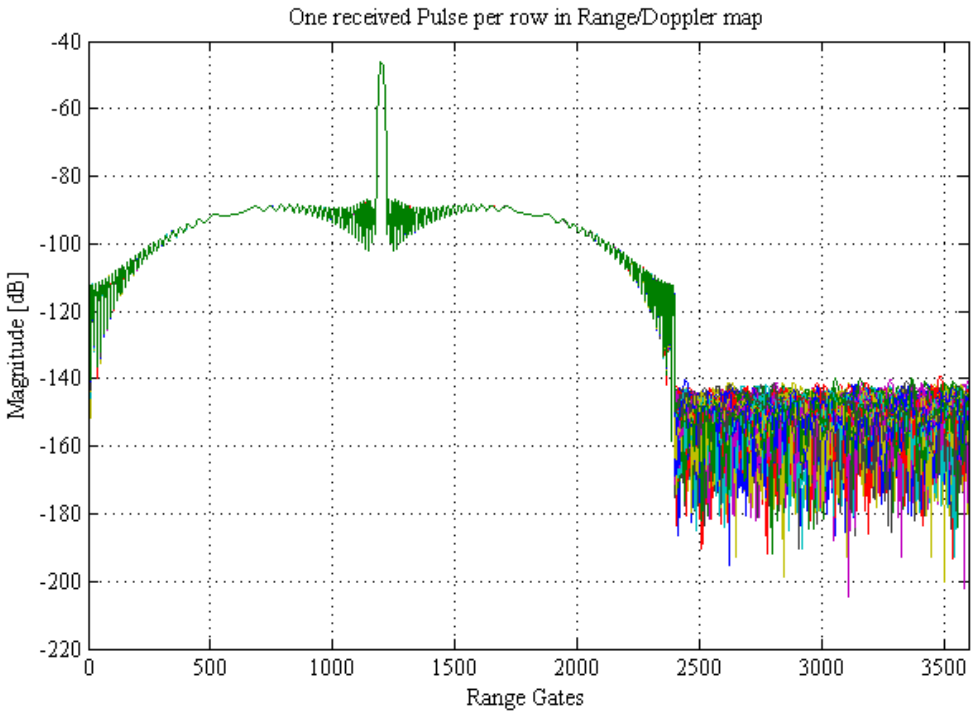

Figure 5.2. *Matched filtering with Hamming weighting*

The Figure 5.2 shows the matched filtering with weighting. After weighting, consider the first matched filtered response of first pulse and the other pulses are placed one above the other as shown in Figure 5.2, the first sidelobe would be 42 dB lower. This is due to the property of hamming window.The magnitude of mainbeam is -46.04 dB and the first side lobe is 40 dB lower than the mainbeam, that is -86.87 dB. Peak Sidelobe Ratio (PSR) and integrated sidelobe ratios are the terms to estimate the sidelobe performance. The PSR can be defined as ratio of peak of the sidelobe to the mainlobe. The PSR is found to be 1.88. The table 5.2 shows the comparison of magnitude of matched filtering response with weighting and without weighting.

Table 5.2. *Matched filtering with weighting and without weighting*

Parameters	Magnitude with weighting [dB]	Magnitude without weighting [dB]
Mainlobe	-46.04	-46.65
First sidelobe	-86.87	-60.09
PSR	1.88	0.776
Sidelobe Level	-40.83	-13.44
Minimum value of Sidelobe	-66.21	-49.94

In Figure 5.3, the matched filtering response for single pulse without weighting is considered, where the magnitude of mainbeam is -46.65 dB and the magnitude of first sidelobe is -60.09 dB and the first peak side lobe level is (-60.09+46.65) =-13.44 dB lower the mainbeam. It is to be observed that in frequency modulated waveform the presence of sidelobes is higher near the mainlobe and the sidelobes gradually decrease from the mainlobe as the distance increases. The minimum sidelobe value or roll-off can be estimated from $-20\log_{10}(\pi B\tau) = -49.94dB$. The integrated side lobe ratio is applicable for multiple targets that can be defined as ratio of sidelobe energy to that of the mainlobe energy. The PSR for this case is found to be 0.776[1].

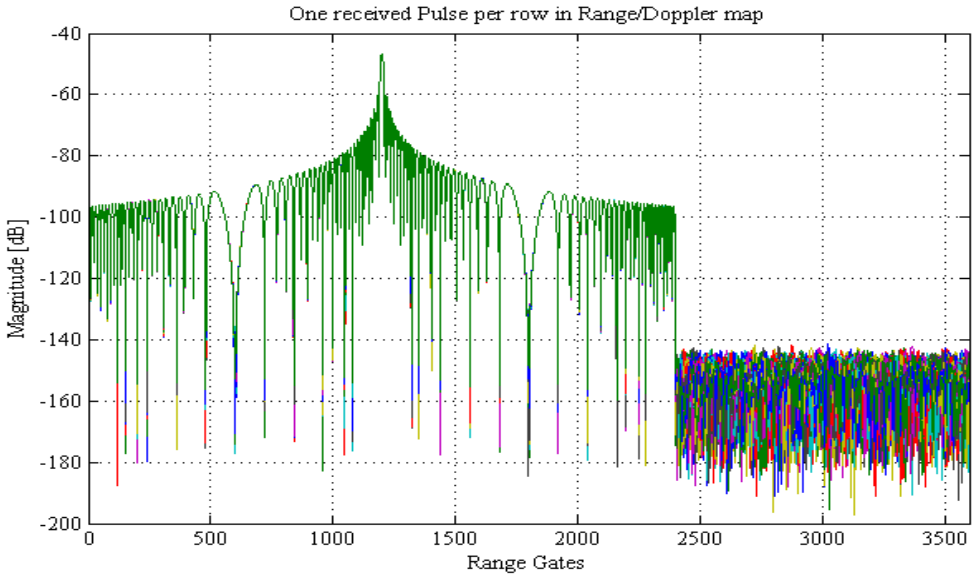

Figure 5.3. *Matched filtering without weighting*

Rayleigh resolution is an important parameter that can be estimated from matched filtering plot. Resolving the scatters that are present closer to each other is termed as Rayleigh resolution. The peak and the first null separation of the matched filter response is the Rayleigh resolution. Thus, the null occurs [1],

$$t = \pm\frac{1}{B} = \pm\frac{1}{10MHz} = 10\mu s \tag{5.3}$$

For two way propagation the Rayleigh resolution can be computed as [1],

$$\delta R = \frac{c}{2B} = 15 \tag{5.4}$$

The improvement in SNR can be computed as [1],

$$(S/N)_{out} = (S/N)_{in} B\tau = 90dB \tag{5.5}$$

where $(S/N)_{in} = 70dB$ is the input of the matched filter, B is the Bandwidth of the LFM signal,τ is the pulsewidth.

5.3. Doppler Processing

The received matched filtered signal is further processed for doppler processing to separate target and clutter. The output of the doppler processing is the R/D matrix where y-axis represents the range gates and x-axis represents the normalized doppler frequency. The matrix or map must be constructed in such a way that there must be one received pulse per row as shown in Figure 5.3. The matrix must have 100 rows and 3601 columns as the number of pulses is 100 and the length of a pulse is 3601. Thus, a matrix size of 100×3601 is generated. As a received pulse is recorded per row, FFT of each column is taken to obtain the corresponding R/D matrix with the location of target and clutter.

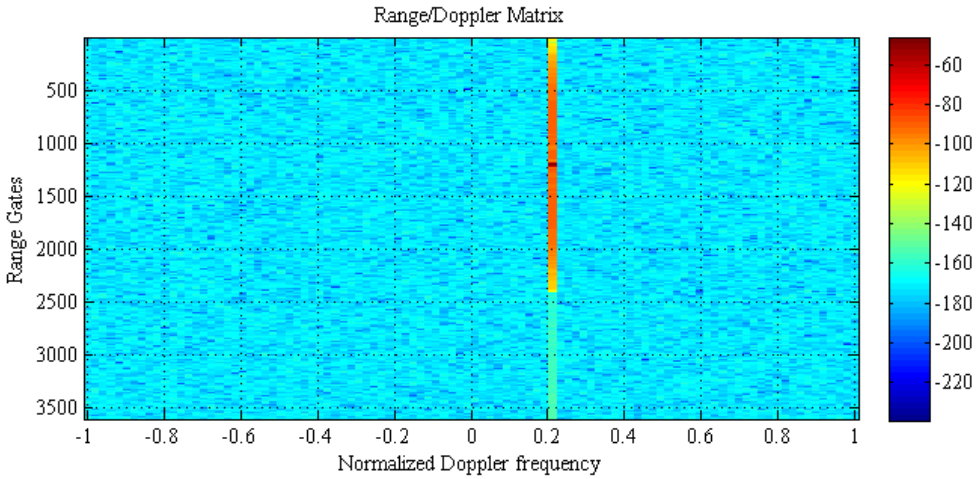

Figure 5.4. *Doppler processing for ideal case with a doppler shift 0.2π*

In the R/D matrix as shown in Figure 5.4, the x-axis represents the normalized doppler frequency, where -1 to 0 represents the negative Doppler frequencies, 0 represents no Doppler and 0 to 1 represents positive Doppler frequencies. Thus, the normalized Doppler frequencies correspond to $(-PRF/2$ to $PRF/2)$ that range from -25μs to 25μs. The colorbar at the right hand side of the Figure 5.4 represents the magnitude of the frequency components produced in the R/ D matrix. If the doppler shift of the target exceeds $PRF/2$, aliasing occurs for every PRF Hz as shown in Figure 5.5. The doppler shift is 0.2π that is present within the range of -1 to 1. If the value of doppler shift is 1.2π, that is greater than 1, aliasing occurs, with the presence of target at -0.8π as shown

in Figure 5.5. This scenario is called the doppler ambiguity as discussed in the section 3.4.2. The estimated value for target radial velocity would be $(-\lambda \times PRF/4, \lambda \times PRF/4)$ $= (-12.5\lambda, 12.5\lambda)$.

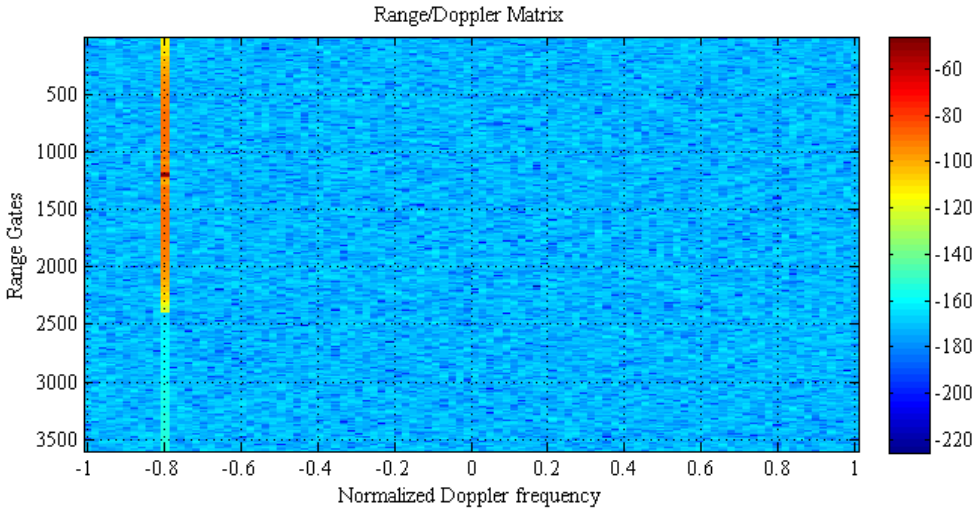

Figure 5.5. *Doppler processing for ideal case with a doppler shift 1.2π*

In ideal case, the presence of clutter and non-linearities are considered to be zero, so that it is easy to analyse the target without non-linearities. The presence of noise is detected in doppler shifts and all ranges and they are constant in nature, termed as noise floor. The channel model for modelling the noise is the AWGN model. It is to be observed from the Figure 5.4, that the target is located at 1200 with a doppler shift of 0.2π. The target is present at the clear region as studied from the topic 3.3.

5.4. Non-Ideal case

The analysis of non-ideal case is carried out in such a way that, the non-linearities are generated at I/Q processing or baseband processing. Thus, the second and third order non-linearities are modelled as illustrated in chapter 4 and the results are obtained as follows.

5.4.1. Effect of Third Order Non-linearities in R/D Matrix

In non-ideal case, third order elements are modelled as shown in (4.28) by introducing third order constants such as $a_3 = 1.5\times10^{-2}$ and $b_3 = 1.5\times10^{-2}$. The constant or weight introduced in I-branch is $a_3 = 1.5\times10^{-2}$ and $b_3 = 1.5\times10^{-2}$ is introduced in Q-branch where memoryless non-linearity is considered. The baseband non-linearity is modelled in the simulator as,

$$y(t) = a_1 x_I(t) + a_3 x_I^3(t) + j\left\{b_1 x_Q(t) + b_3 x_Q^3(t)\right\} \tag{5.6}$$

where $x_I(t)$ and $x_Q(t)$ are the signals in I-branch and Q-branch. The following simulations are simulated and the following observations are made.

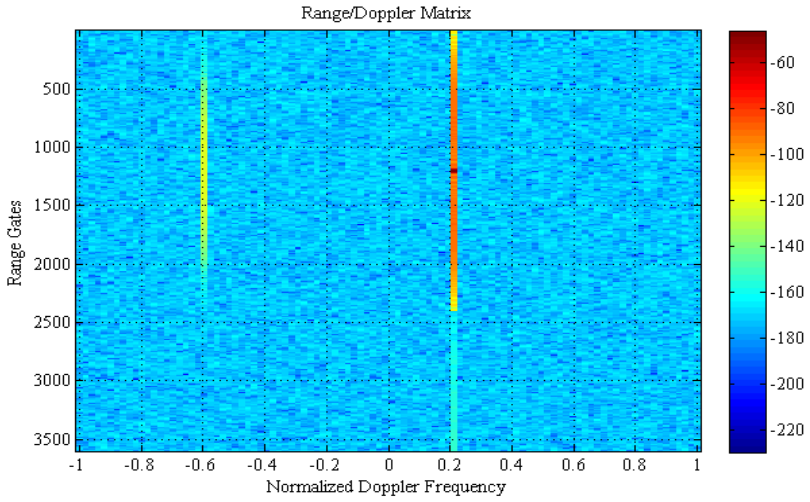

Figure 5.6. *Doppler processing for third order nonlinearity with doppler shift* 0.2π

From the R/D matrix as shown in Figure 5.6, the orginal doppler frequency of the target is 0.2π. As the orginal doppler frequency is 0.2π, the third order frequency component $3f_d$ should produce new frequency component $3\times0.2\pi=0.6\pi$ but the frequency component would fall at negative doppler region, -0.6π as the third order distortion component would fall opposite to that of the location of the target signal. The target signal has additional spurious frequency component (also called self distortion component) at the doppler frequency 0.2π. Thus, the target signal is affected by the self distortion component, affecting the desired bandwidth. Thus, it holds for all the odd order components (3, 5 ...). On comparing the R/D matrix obtained in Figure 5.6 to that of the modelling of the third order non-linearity in equation (4.29), table 5.3 is obtained as shown below.

Table 5.3. *Third order distortion profile in R/ D Matrix*

Third order Distortion Profile	**Frequency components**	**Normalized Doppler Frequency**
Target Signal	$b_1A(t)\exp(j(\omega_a t+\phi(t)+\varphi_0))$	0.2π
Self Distortion component	$\frac{3}{4}b_3A^3(t)\exp(j(\omega_a t+\phi(t)+\varphi_0))$	0.2π
Third order Frequency component ($-3\omega_a$)	$\frac{1}{4}b_3A^3(t)\exp(-j(3\omega_a t+3\phi(t)+3\varphi_0))$	-0.6π

In a pulse doppler system, for easy target detection and tracking, the circuits that are involved in signal processing, timing signals and reference signals play an important role and these circuits must be stable. The stability of radar can be analyzed by two methods. They are short term stability and long term stability. The thesis mainly focuses on long term stability that deals with mostly on spurious signals for range and velocity accuracy where it is easy to satisfy the requirement. Variations in round trip echo signal time mostly focussed in short term stability [10].

The next case is to analyse the change in doppler frequency of the target with third order non-linearities. Let the target be placed at doppler frequency at 0.4π. The third order non-linearities are modelled and effects are observed in R/D matrix as shown in Figure 5.7. It is to be observed from the Figure 5.7 that third order component is produced at 0.8π. The third order non-linearities produce new frequency components at $-3f_d$ and a selfdistortion component at f_d. Thus, the new frequency component would be placed at negative Doppler region -1.2π as it exceeds the range -1 to 1. But the frequency component at -1.2π would cause aliasing at positive Doppler region 0.8π. Thus, aliasing occurs as the target exceeds the doppler frequency. The Figure 5.7 shows the doppler ambiguity with the effect of third order distortion.

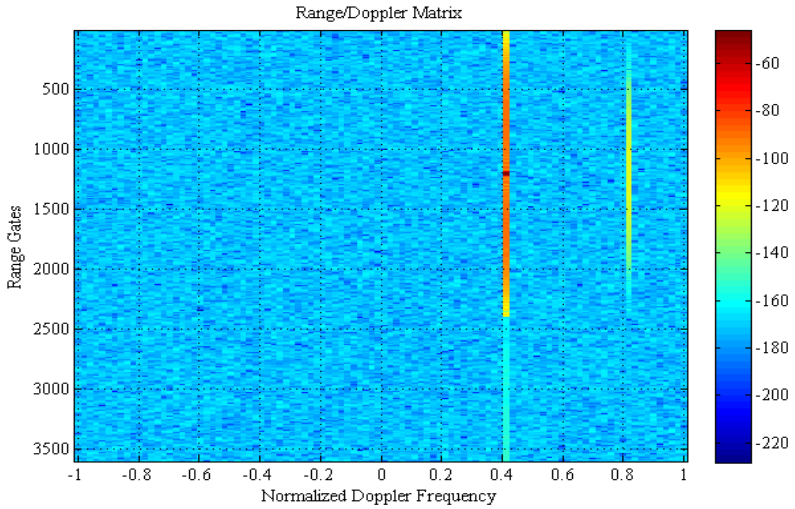

Figure 5.7. *Doppler processing for third order nonlinearity with doppler shift* 0.4π

The next case of analysis is to introduce some differences in modelling of third order non-linearities in I and Q branches. To model, it assumed that, difference between the weights in I and Q branches is 0.5×10^{-2} where $a_3=1.5\times10^{-2}$ and $b_3=1\times10^{-2}$. The constant or weight $a_3=1.5\times10^{-2}$ is introduced in modelling third order distortion in I- branch and $b_3=1\times10^{-2}$ is introduced in modelling third order distortion in Q-branch. Thus, the scenario is not realistic as there would be some imbalance in first order terms.

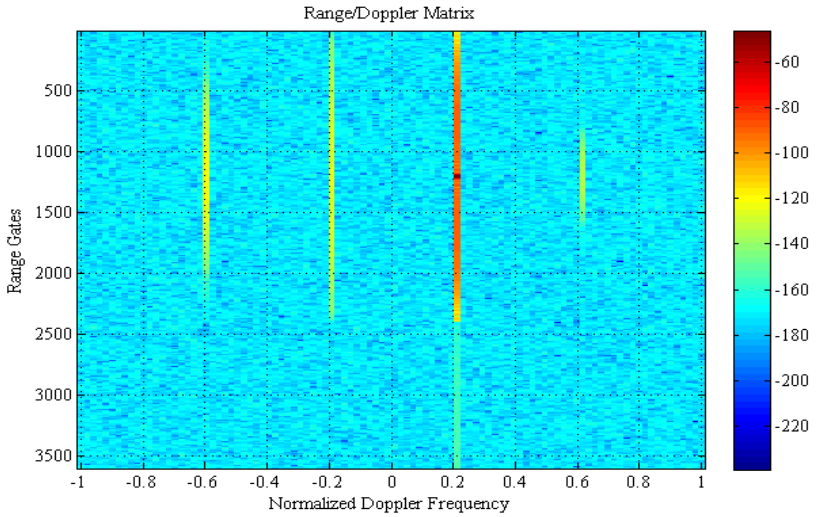

Figure 5.8. *Doppler processing for third order nonlinearity with I/Q imbalance*

On introducing (4.32) in the simulator, the effect of third order non-linearities with imbalance in I and Q branches are observed. In R/D matrix as shown in Figure 5.8, the target is placed at doppler frequency 0.2π. Due to the effect of third order non-linearity, a new frequency component is produced at -0.6π, that is found to be at negative doppler region. As there is imbalance in I and Q branches, conjugate mirror image of the target and new frequency component are produced. The conjugate mirror image of the target is due to the self-distortion component present in the target signal. The self-distortion component in the target signal at 0.2π produces mirror image at -0.2π. It is also found that, due to the effect of imbalance, a mirror image of the third frequency component (at -0.6π) falls at positive doppler region 0.6π. Thus, the scenario is not realistic, as there would be some imbalance in first order terms. On introducing some imbalance in first order terms, other than the mirror image of the self-distortion component, mirror image of the target signal is obtained at -0.2π. Thus, there would be higher effects of third order distortion if there is imbalance in first order terms. On comparing the R/D matrix as obtained in Figure 5.8 to that of the equation (4.33), the following table 5.4 is obtained.

Table 5.4. *Third order distortion profile with I/ Q imbalance in R/ D Matrix*

Third order Distortion Profile	Frequency components	Normalized Doppler frequency
Target Signal	$b_1 \frac{1+g_1}{2} A(t)\exp(j(\omega_a t+\phi(t)+\varphi_0))$	0.2π
Mirror image of target signal	$b_1 \frac{1-g_1}{2} A(t)\exp(-j(\omega_a t+\phi(t)+\varphi_0))$	-
Self Distortion component	$\frac{3}{4} b_3 \frac{1+g_3}{2} A^3(t)\exp(j(\omega_a t+\phi(t)+\varphi_0))$	0.2π
Mirror image of self distortion component	$b_3 \frac{1-g_3}{2} A^3(t)\exp(-j(\omega_a t+\phi(t)+\varphi_0))$	-0.2π
Third order Frequency component ($+3\omega_a$)	$\frac{1}{4} b_3 \frac{1-g_3}{2} A^3(t)\exp(j(3\omega_a t+3\phi(t)+\varphi_0))$	-0.6π
Mirror image of Third order Frequency component ($-3\omega_a$)	$b_3 \frac{1+g_3}{2} A^3(t)\exp(-j(3\omega_a t+3\phi(t)+\varphi_0))$	0.6π

5.4.2. Effect of Second Order Non-linearities in R/D Matrix

In non-ideal case, second order elements are modelled as shown in (4.24) by introducing order constants such as $a_2 = 1.5\times10^{-2}$ and $b_2 = 1.5\times10^{-2}$. The constant or weights $a_2 = 1.5\times10^{-2}$ is introduced in I-branch and $b_2 = 1.5\times10^{-2}$ is introduced in Q-branch where memoryless non-linearity is considered. The baseband non-linearity is modelled as,

$$y(t) = a_1 x_I(t) + a_2 x_I^2(t) + j\left\{b_1 x_Q(t) + b_2 x_Q^2(t)\right\} \tag{5.7}$$

where $x_I(t)$ and $x_Q(t)$ are the signals in I-branch and Q-branch. The following simulations are simulated and the following observations are made.

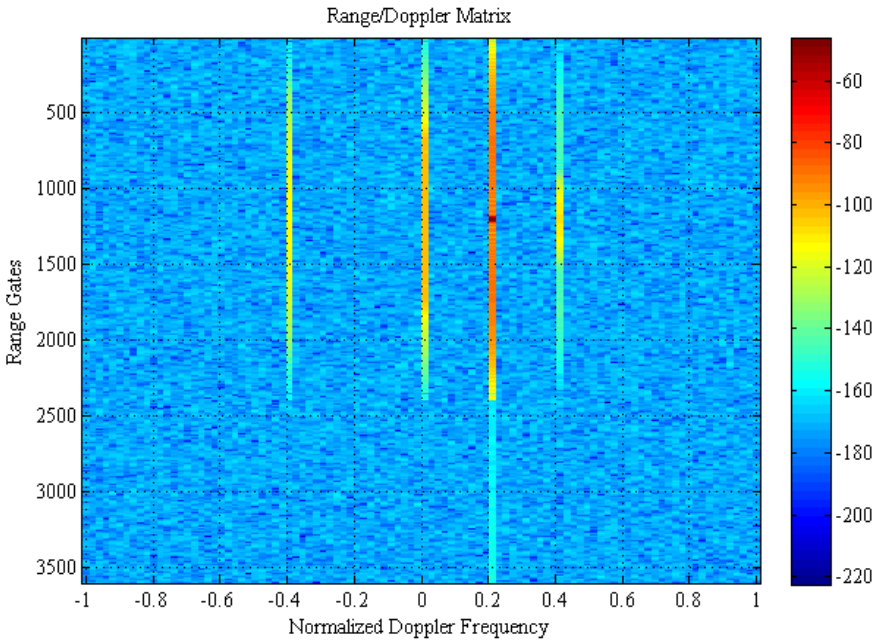

Figure 5.9. *Doppler processing for second order nonlinearity with doppler shift* 0.2π

The Figure 5.9 shows the R/D matrix, after introducing the second order non-linearities. The target is placed at a positive doppler frequency of 0.2π. Thus, it is to be observed that second order frequency components are produced at $+2f_d$ and $-2f_d$. Thus, the corresponding second order frequency components are $+0.4\pi$ and -0.4π. A DC component is also generated at doppler region 0. On comparing the Figure 5.9 with Figure 5.6, the resolution of the target is better in Figure 5.9 as the target signal is free from self-distortion component. On increasing the even order distortion components, similar symmetry is obtained.

It is to be noted that, a main difference exists between the second and third order model. In some cases, the third order model is more prone to spurious responses than the second order model by affecting the desired bandwidth. On comparing the R/D matrix as obtained in Figure 5.9 to that of the equation (4.27), the following table 5.5 is obtained.

Table 5.5. *Second order distortion profile in R/D Matrix*

Second order Distortion Profile	**Frequency components**	**Normalized Doppler Frequency**
Target signal	$b_1 A(t)\exp(j(\omega_a t+\phi(t)+\varphi_0))$	0.2π
DC Component	$\frac{1}{2}(1+j)b_2 A^2(t)$	0
Second order frequency component at $+2\omega_a$	$\frac{1}{4}(1-j)b_2 A^2(t)\exp(j(2\omega_a t+2\phi(t)+\varphi_0))$	0.4π
Second order frequency component at $-2\omega_a$	$\frac{1}{4}(1-j)b_2 A^2(t)\exp(-j(2\omega_a t+2\phi(t)+\varphi_0))$	-0.4π

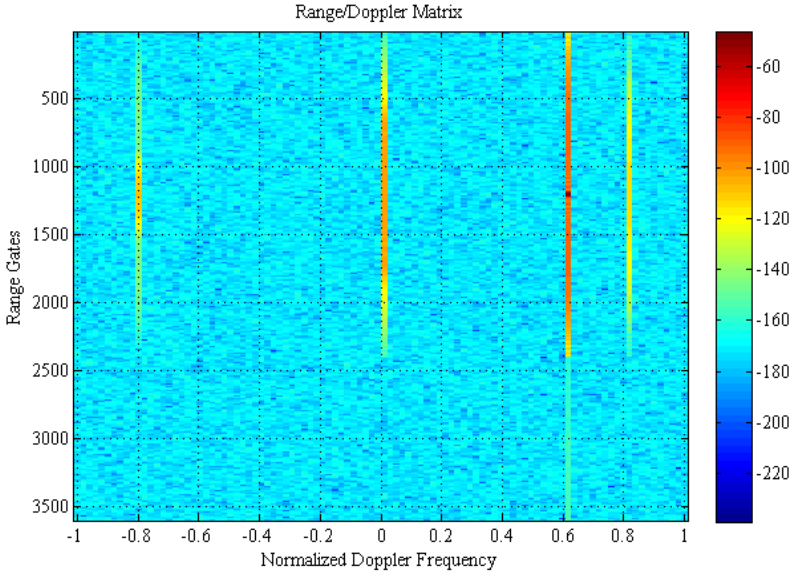

Figure 5.10. *Doppler processing for second order nonlinearity with doppler shift* 0.6π

The next case is to analyse the effect of increase in doppler frequency of the target. The target is placed at the doppler frequency 0.6π. As the second order components produces two frequency components $+2f_d$ and $-2f_d$, the corresponding frequency components are $+1.2\pi$ and -1.2π. As the second order frequency component exceeds the range –PRF/2 to PRF/2, aliasing occurs, thus producing frequency components at $+0.8\pi$ and -0.8π. Also a DC component at Doppler region is produced similar to the previous case as shown in Figure 5.10. Thus, Figure 5.10 shows the doppler ambiguity with the effect of second order distortion.

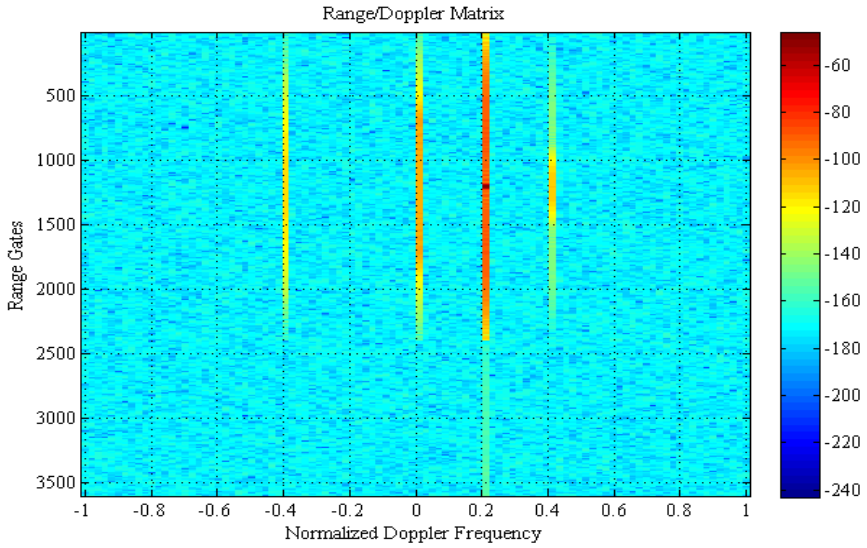

Figure 5.11. *Doppler processing for second order nonlinearity with I/Q imbalance*

On introducing (4.30) in the simulator, the effect of second order non-linearities with imbalance in I and Q branches are observed. On considering the R/D matrix as shown Figure 5.11, further development of the signal modelling is implemented by introducing some difference in the behaviour of I and Q branches. To model this, it is assumed that the weights in I branch as $a_2 = 1.5\times10^{-2}$ and weights in Q-branch as $b_2 = 1\times10^{-2}$. It is to be observed that, the location of target signal is 0.2π producing, second order frequency components at 0.4π and -0.4π. Thus, mirror image of the frequency component 0.4π is produced at -0.4π and mirror image of the frequency component -0.4π is produced at 0.4π. A DC component is produced at doppler region 0. It is known that the second order distortion do not have the presence of self distortion component in the desired target signal. Thus, no mirror image of the self-distortion component is produced. Thus, the scenario is not realistic, as there would be some imbalance in first order terms. On introducing some imbalance in first order terms, mirror image of the target signal is obtained at -0.2π. Thus, there would be higher effects of second order distortion if there is imbalance in first order terms. On comparing the R/D matrix as obtained in Figure 5.11 to that of the equation (4.31), the following table 5.6 is obtained.

Table 5.6. *Second order distortion profile with I/ Q imbalance in R/ D Matrix*

Second Order Distortion Profile	**Frequency Component**	**Normalized Doppler Frequency**
Target Signal	$b_1\frac{1+g_1}{2}A(t)\exp(j(\omega_a t+\phi(t)+\varphi_0))$	0.2π
Mirror image of target signal	$b_1\frac{1-g_1}{2}A(t)\exp(-j(\omega_a t+\phi(t)+\varphi_0))$	-
DC Component	$\frac{1}{2}(1+jg_2)b_2A^2(t)$	0
Second order frequency component at $+2\omega_a$	$\frac{1}{4}(1-jg_2)b_2A^2(t)\exp(j(2\omega_a t+2\phi(t)+2\varphi_0))$	0.4π
Second order frequency component at $-2\omega_a$	$\frac{1}{4}(1-jg_2)b_2A^2(t)\exp(-j(2\omega_a t+2\phi(t)+2\varphi_0))$	-0.4π

6. CONCLUSION

The concept of coherency is foremost important aspect of the thesis. As the thesis deals with the term ‘Doppler’ the work is carried out such that the transmitter and receiver are assumed to be coherent in nature. The phase is assumed to be same from pulse to pulse as the pulse doppler radar is coherent radar. Thus, coherent radars extract both range and doppler whereas the non-coherent radar can extract range only.

The DCR in radar has been implemented by deploying quadrature downconversion principle. The signal at the baseband is studied, to look into the effect of non-linearities that is generated at I and Q branches. Thus, the baseband non-linearities are implemented in this thesis. The third order distortion effect seems to be crucial, as the third order products are closer to the desired signal and produce self-distortion terms affecting the desired target signal thereby masking the target. Thus, the study has also led to the understanding on the effect of doppler in radar with the aid of R/D matrix. The effect of ambiguities such as doppler ambiguity that produces aliasing or foldover effect is also studied. Thus, it is very important to study about the effect of non-linearities in radar as it helps to study about the radar performance.

The effect of second order non-linearity, third order non-linearity and ambiguities can be observed in the post-processing blocks such as matched filtering or pulse compression and doppler processing.The importance of hamming weight is illustrated in the results by comparing the matched filtering response with and without weighting. Thus, fine range resolution is obtained, thereby suppressing the sidelobes in the matched filtering response. LFM also called chirp is the pulse compression technique implemented due to the ease in generating the signal and its insensitivity to doppler shifts. R/D matrix is the output of the pulse doppler processing in a pulse doppler radar. Parameters such as range, doppler information are obtained from the doppler processing as illustrated in the analysis. A further step in post-processing can be implemented using Constant False Alarm Rate Algorithm (CFAR) to identify target hits (0 or 1) by generating a threshold.

The study can be further extended by implementing DSP techniques for mitigating the baseband non-linearities, but it is essential to study the non-ideality effects in the radar receiver. For designing the proper compensation structure it is necessary to understand the effect of non-linear distortion as discussed in the thesis. Thus, for discussing the effect of non-linear distortion, the baseband non-linearities are modelled and the received echo signal with doppler are introduced into the simulator. From the mathematical expression, the effect of doppler on the received signal at baseband is analysed. Other than the baseband non-linearities the study can be further extended to RF non-linearities and effect of jammers affecting the desired signal. There exists a DC compo-

nent in the second order distortion profile as discussed in the results. Thus, possible future research can be implemented on the study of effect of DC offset and phase noise with corresponding mitigation algorithms. By considering more than one received signal from more than one target (multiple target scenario), possible cross- modulation terms can be generated for illustrating the concept of cross modulation in radar receivers.

.

REFERENCES

[1] Richards, M.A., Scheer, J.A. and Holm, W.A. Principles of Modern Radar, vol.1, 2010, *Scitech Publishing Inc*.

[2] Dufrene, R. Recent Advances in Radar Technology in Telecommunication Research Institute, Vol.3, 2000, *Telecommunications Research Institute, Microwaves, Radar and Wireless Communications.MIKON-2000, 13th International Conference*, pp. 230-236.

[3] Litrenta, T. Advances in Radar Processing, *Military Aerospace Electronics*, 2008. [Accessed on 5.01.2013]. Available at: *http://www.militaryaerospace.com/articles/print/volume-19/issue-6/departments/opinion/advances-in-radar-processing.html*

[4] Shahed hagh ghadam, A., Valkama, M. and Renfors, M. Adaptive Compensation of Nonlinear Distortion in Multicarrier Direct Conversion Receivers, 2004, *IEEE*, pp. 35-38.

[5] Valkama, M., Shahed hagh ghadam, A., Anttila, L. and Renfors, M. Advanced Digital Signal Processing Techniques for Compensation of Nonlinear Distortion in Wideband Multicarrier Radio Receivers, 54(2006)6, *IEEE Transactions on Microwave Theory and Techniques.*

[6] Valkama, M., Renfors, M. and Koivunen, V. Advanced Methods for I/Q Imbalance Compensation in Communication Receivers, 49(2001)10, *IEEE Transactions on Signal Processing.*

[7] Shahed hagh ghadam, A. Contributions to Analysis and DSP-based Mitigation of Nonlinear Distortion in Radio Transceivers, *Doctoral Thesis*, Tampere, 2011, TUT, 122p.

[8] Vallant, G., Epp, M., Schlecker, W., Schneider, U., Anttila, L. and Valkama, M. Analog IQ Impairments in Zero- IF Radar Receivers: Analysis, Measurements and Digital Compensation, 2012, *Instrumentation and Measurement Technology Conference (I2MTC), IEEE International*, pp. 1703-1707.

[9] Christensen, E.L, Madsen, S.N. and Skou, N. Review of the Homodyne Technique for Coherent Radar, July 05 2010, *IEEE International Radar Conference*, pp. 159-163.

[10] Skolnik, M. Radar Handbook, Third Edition, 2008, *McGraw Hill*, 1352p.

[11] Mahafza, B.R. Radar Signal Analysis and Processing using Matlab, 2009, *CRC Group*, 479p.

[12] Hansen, V.G. Topics in Radar Signal Processing, Part 1: Overview and Coherent Processing Techniques, March 1984, *Microwave Journal*, pp. 24-36.

[13] Wiesbeck, W. Radar System Engineering, 13th Edition, Germany, 2006/2007, *Universitat Karlsruhe (TH)*, 162p.

[14] Mudukutore, S.A., Chandrasekar, V., and Keeler, J. Pulse Compression on Weather Radars, 36(1998)1, *IEEE Transactions on Geoscience and Remote Science*, pp. 125-142.

[15] Varshney, L.R. andThomas, D. Sidelobe Reduction for Matched Filter Range Processing, 2003, *IEEE Radar Conference*, pp. 446-450.

[16] Harris, F.J. On the Use of Windows for Harmonic Analysis with the Discrete Transform, 66(1978)1, *Proceedings of the IEEE*, pp. 51-83.

[17] Mirabbasi, S. and Martin, K. Classical and Modern Receiver Architectures, Nov. 2000, *IEEE Communications Magazine*, pp.132-139.

[18] Razavi, B. Design Considerations for Direct-Conversion Receivers, 44(1997)6, *IEEE Transactions on Circuits and Systems-II: Analog and Digital Signal Processing*, pp. 428-435.

[19] Ming, L.I., Yu-Mei, L. and Feng, R. A Simple Simulation Method Ground Clutter for Airborne Pulse Doppler Radar, 2006, *IEEE*.

[20] Kim, S.J., Ju, Y.H. and Hun, J. Design and Implementation of a Full- Digital Pulse-Doppler Radar System for Automotive applications, 2011, *IEEE International Conference on Consumer Electronics (ICCE)*, pp. 563-564.

[21] Rasool, B.S. and Bell, R.B. Efficient Pulse- Doppler Processing and Ambiguity Functions of Non-uniform Coherent Pulse Trains, 2010, *IEEE*, pp. 001150-001155.

[22] Venter, C.J., Grobler, H. and AlMalki, K.A. Implementation CA-CFAR Algorithm for Pulsed-Doppler Radar on a GPU Architecture, 2011, *IEEE Jordan Conference on Applied Electrical Engineering and Computing Technologies (AEECT)*.

[23] Broich, R. and Grobler, H. Analysis and Computational Requirements of a Pulse- Doppler Radar Signal Processor, 2012, *IEEE Radar Conference*.

[24] Springer. Radar Fundamentals. 2012, *Millimeter- Wave Receiver Concepts for 77 GHz Automotive*, pp. 9-19.

[25] Levanon, N. and Mozeson, E. Radar Signals, 2004, *John Willey and Sons Inc.*

[26] Wolff, C. Radar Tutorial. Available at: *www.radartutorial.eu*

[27] Ahn, S., Lee, H. and Jung, B. Medium PRF set Selection for Pulsed Doppler Radars using Simulated Annealing, 2011, *IEEE*.

[28] Huabing, X., Quanxia, M. and Wei, P. Pulse Doppler Radar based on Adaptive Genetic Algorithm, 2011, *IEEE Chinese Control and Decision Conference (CCDC)*, pp. 31-34.

[29] Faulkner, M. DC Offset and IM2 removal in Direct Conversion Receivers, 149(2002)3, *IEEE Proceedings*, pp. 179-184.

[30] Agilent Radar Measurements, Agilent Technologies, 78p.

[31] Syrjala, V. Analysis and Mitigation of Oscillator Impairments in Modern Receiver Architectures, *Doctoral Thesis*, Tampere 2012, TUT, 88p.

A. APPENDIX

The below Figure A.1 shows the overall matched filtering response for hundred pulses.

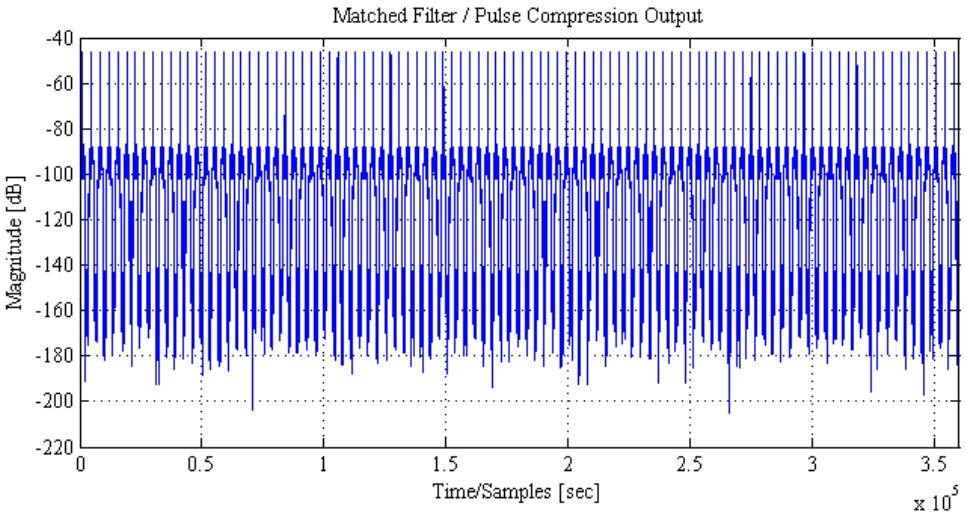

Figure A.1. *Matched Filtering response for hundred pulses*